iScience

CellPress
OPEN ACCESS

Article

Identification of a Quorum Sensing-Dependent Communication Pathway Mediating Bacteria-Gut-Brain Cross Talk

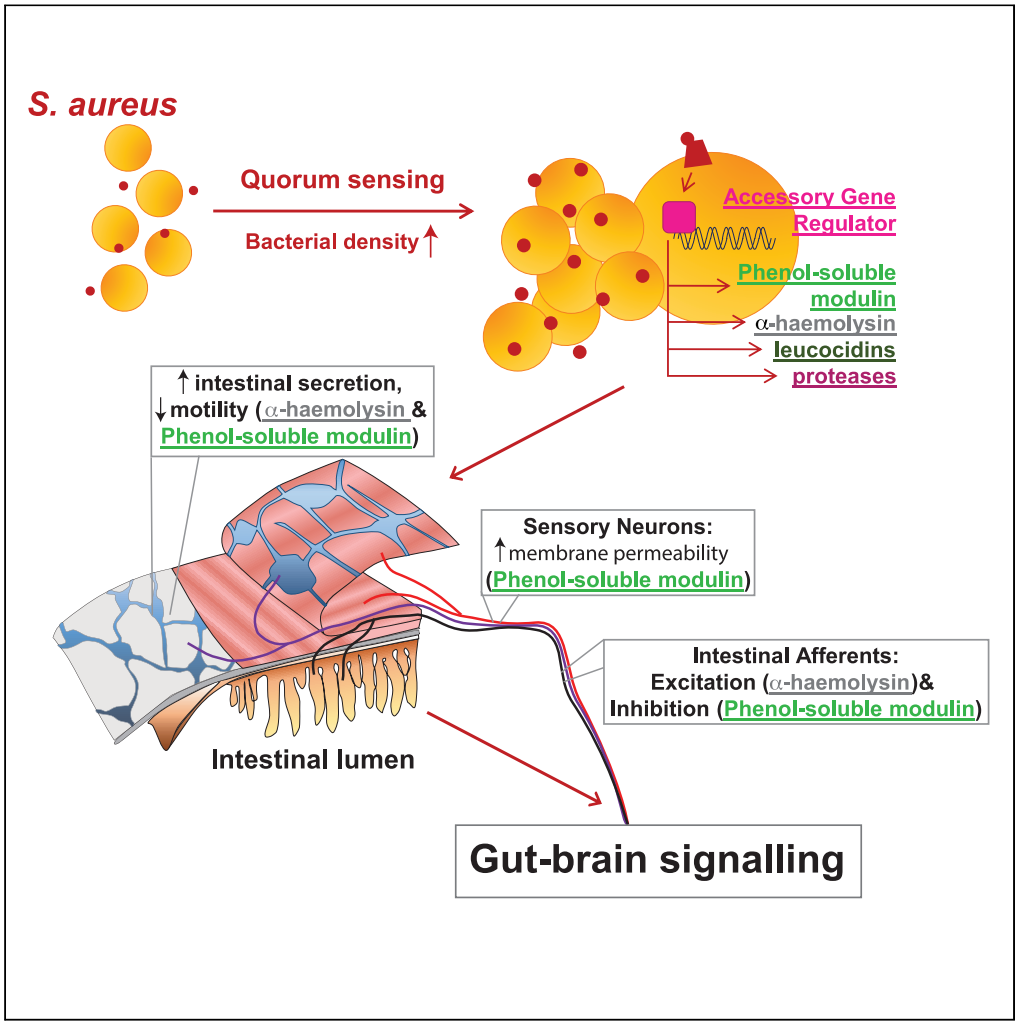

Friederike Uhlig, Luke Grundy, Sonia Garcia-Caraballo, Stuart M. Brierley, Simon J. Foster, David Grundy

d.grundy@sheffield.ac.uk

HIGHLIGHTS

Quorum sensing-regulated secretions modulate intestinal neurons, secretion, and motility

Intestinal neurons are able to "sense" bacteria independently of the host immune system

Excitation and inhibition of intestinal afferents is mediated by pore-forming toxins

Bacterial mediators directly influence microbiota-gut-brain axis signaling pathways

Uhlig et al., iScience 23, 101695
November 20, 2020
https://doi.org/10.1016/j.isci.2020.101695

iScience

CellPress
OPEN ACCESS

Article

Identification of a Quorum Sensing-Dependent Communication Pathway Mediating Bacteria-Gut-Brain Cross Talk

Friederike Uhlig,[1] Luke Grundy,[2,3,4] Sonia Garcia-Caraballo,[2,3,4] Stuart M. Brierley,[2,3,4] Simon J. Foster,[5,6] and David Grundy[1,7,*]

SUMMARY

Despite recently established contributions of the intestinal microbiome to human health and disease, our understanding of bacteria-host communication pathways with regard to the gut-brain axis remains limited. Here we provide evidence that intestinal neurons are able to "sense" bacteria independently of the host immune system. Using supernatants from cultures of the opportunistic pathogen *Staphylococcus aureus* (*S. aureus*) we demonstrate the release of mediators with neuromodulatory properties at high population density. These mediators induced a biphasic response in extrinsic sensory afferent nerves, increased membrane permeability in cultured sensory neurons, and altered intestinal motility and secretion. Genetic manipulation of *S. aureus* revealed two key quorum sensing-regulated classes of pore forming toxins that mediate excitation and inhibition of extrinsic sensory nerves, respectively. As such, bacterial mediators have the potential to directly modulate gut-brain communication to influence intestinal symptoms and reflex function *in vivo*, contributing to homeostatic, behavioral, and sensory consequences of infection.

INTRODUCTION

Neurons of the peripheral nervous system play important roles in the detection of potentially harmful stimuli. Activation of specialized somatosensory fibers in the skin by such stimuli initiates pain and escape reflexes (Woolf, 2018). Visceral sensory neurons transmit information from the internal organs to the brain and have important functions in the regulation of homeostasis, food intake, mood, and memory (Furness et al., 2013; Lai et al., 2017). Symptoms of neuronal dysfunction such as illness, behavior, and chronic visceral pain, are frequently associated with infections (Brierley and Linden, 2014). Until recently, it was thought that such dysfunction resulted from an over- or inappropriate activation of the immune system. In this scenario, mediators released from immune cells during inflammation activate sensory neurons signaling to the brain and spinal cord (Hughes et al., 2013; Campaniello et al., 2017). Although this mechanism undoubtedly contributes to the late stages of inflammation, recent studies suggest that somatosensory pain during the early stages of infection correlates with bacterial load and results from a direct interaction between bacteria and neurons independent of the inflammatory response (Chiu et al., 2013; Blake et al., 2018).

The gastrointestinal (GI) tract constitutes a large reservoir of bacteria, viruses, archaea, and fungi, which is also known as the microbiome. These microbes have the potential to interact with visceral sensory neurons, especially if there is a breakdown in the mucosal epithelial barrier, as occurs in disease (David et al., 2014; Kelly et al., 2017). In addition to these extrinsic neurons, the intestine is densely innervated by neurons of the enteric nervous system that are important for the regulation of intestinal motility and secretion (Furness et al., 2013). The extent to which bacterial mediators directly interact with either of these populations of intestinal neurons is not known. A direct interaction of bacterial metabolites with sensory neurons, however, could not only contribute to the diverse neuronal symptoms during bacterial infections but also mediate pathophysiological consequences of changes of the microbiome composition (Fülling et al., 2019).

Studies investigating the neuromodulatory potential of substances produced by bacteria have largely focused on cell-wall components. Lipopolysaccharide, polysaccharide A, and peptidoglycans from *Lactobacillus* and *Bacteroides* species have been shown to increase enteric neuronal excitability and intestinal

[1]Department of Biomedical Science, University of Sheffield, Sheffield, UK

[2]Visceral Pain Research Group, College of Medicine and Public Health, Flinders Health and Medical Research Institute (FHMRI), Flinders University, Bedford Park, SA, Australia

[3]Hopwood Centre for Neurobiology, Lifelong Health Theme, South Australian Health and Medical Research Institute (SAHMRI), North Terrace, Adelaide, SA, Australia

[4]Discipline of Medicine, University of Adelaide, Adelaide, SA, Australia

[5]Department of Molecular Biology and Biotechnology, University of Sheffield, Sheffield, UK

[6]Florey Institute, University of Sheffield, Sheffield, UK

[7]Lead Contact

*Correspondence: d.grundy@sheffield.ac.uk

https://doi.org/10.1016/j.isci.2020.101695

motility (Wang et al., 2010; Mao et al., 2013). These bacteria also affect brain activation patterns, as well as emotional and exploratory behavior (Bercik et al., 2011; Bravo et al., 2011; Bharwani et al., 2020). However, cell-wall glycolipids are not alone in mediating the effects of commensal and pathogenic strains of bacteria contributing to neuronal symptoms of infection and intestinal dysbiosis. Different strains produce largely different exoproteomes and metabolites depending on their genetic background and environmental cues via quorum sensing (QS) (Chapman et al., 2017; Burgui et al., 2018). *Staphylococcus aureus* (*S. aureus*) is particularly rich in the variety of virulence factors it secretes to manipulate the host's immune response and ensure bacterial survival (Tam and Torres, 2019). QS refers to the process of bacteria-to-bacteria communication, and because of the high bacterial density in the intestine, QS-regulated bacterial mediators are likely to play an important role in gut signaling.

QS-regulated genes are usually activated at high bacterial density and include pathogenicity-related genes such as exotoxins (Mukherjee and Bassler, 2019). Exotoxins have long been studied for their immunogenic role (Los et al., 2013) but more recently have also been shown to be instrumental in pain hypersensitivity during *S. aureus* and *Streptococcus pneumonia* infection (Chiu et al., 2013; Blake et al., 2018). In *S. aureus*, QS activates the transcription factor Accessory gene regulator (Agr)A, which regulates the expression of a number of genes. This includes virulence factors such as formylated peptides, pore-forming toxins (PFTs) (hemolysins, leucocidins, and phenol-soluble modulins) and bacterial proteases (Wang et al., 2007). These toxins were shown to increase intracellular calcium and action potential firing in cultured sensory neurons (Chiu et al., 2013; Blake et al., 2018). The importance of such exotoxins for intestinal physiology and gut-brain communication, however, is currently unknown.

S. aureus is an opportunistic pathogen that is present in about one-third of the population. It is well recognized as a skin and nose bacterium, but reports show that the GI tract is a major reservoir that is thought to increase the risk for recurrent infection (Chang and Lin, 2016). A particularly high prevalence has been reported for hospitalized patients including children in neonatal intensive care (Acton et al., 2009; Nakao et al., 2014). Because *S. aureus* has also been associated with irritable bowel syndrome and food poisoning (Rinttilä et al., 2011; Denayer et al., 2017), we hypothesized that *S. aureus* modulates intestinal neuron activity. Our objective was to use supernatants from *S. aureus* cultures to determine the effect on intestinal function and signaling. Using a genetic approach, with access to a library of *S. aureus* mutants, we identified a pivotal role for the Agr. Agr-regulated mediators had distinct effects on afferent nerve activity. The PFT α-hemolysin (Hla) contributed to *S. aureus* supernatant-induced excitation, whereas phenol-soluble modulins were found to predominantly drive inhibition. These and other mediators were also involved in the effects of *S. aureus* supernatants on intestinal secretion and motility.

RESULTS

Modulation of Intestinal Afferent Sensitivity by Soluble Mediators from *S. aureus*

Small intestinal afferents generate action potentials spontaneously in the absence of additional stimulation. Bath application of 20% v/v supernatants of cultures from *S. aureus* (SSA) induced a biphasic afferent response with an initial excitation followed by profound inhibition (Figure 1A). The increase in nerve activity was maximal until about 30 min after supernatant application and was followed by inhibition after 60 min, which in many cases resulted in complete silencing of afferent firing. Bacteria-free growth medium (BF-GM) was used as a vehicle control and resulted in a small degree of excitation that was significantly below that caused by SSA and persisted for the duration of the experiment, with no apparent inhibition (Figures 1B and S1A). This observation is consistent with SSA containing a number of mediators that cause excitation and/or inhibition of afferent firing.

Next, we determined the extent to which excitation and inhibition were dependent on mediator concentration. With 10% v/v SSA, the response profile was similar to that seen at 20% v/v (Figure 1B). Both, excitation and inhibition were not significantly different to 20% SSA. Bath application of 5% SSA induced a level of excitation that was comparable to 10% and 20% SSA; however, the inhibitory effect was significantly reduced (Figure 1B). As excitation but not inhibition was supramaximal at 5%, this suggests that they are mediated by different mediators within SSA.

In addition to spontaneous activity, afferent discharge of small intestinal afferents can be evoked by luminal distension as a result of the activation of distinct populations of low- and high-threshold fibers (Rong et al., 2004). We investigated the effect of SSA on mechanosensitive intestinal afferent fibers by

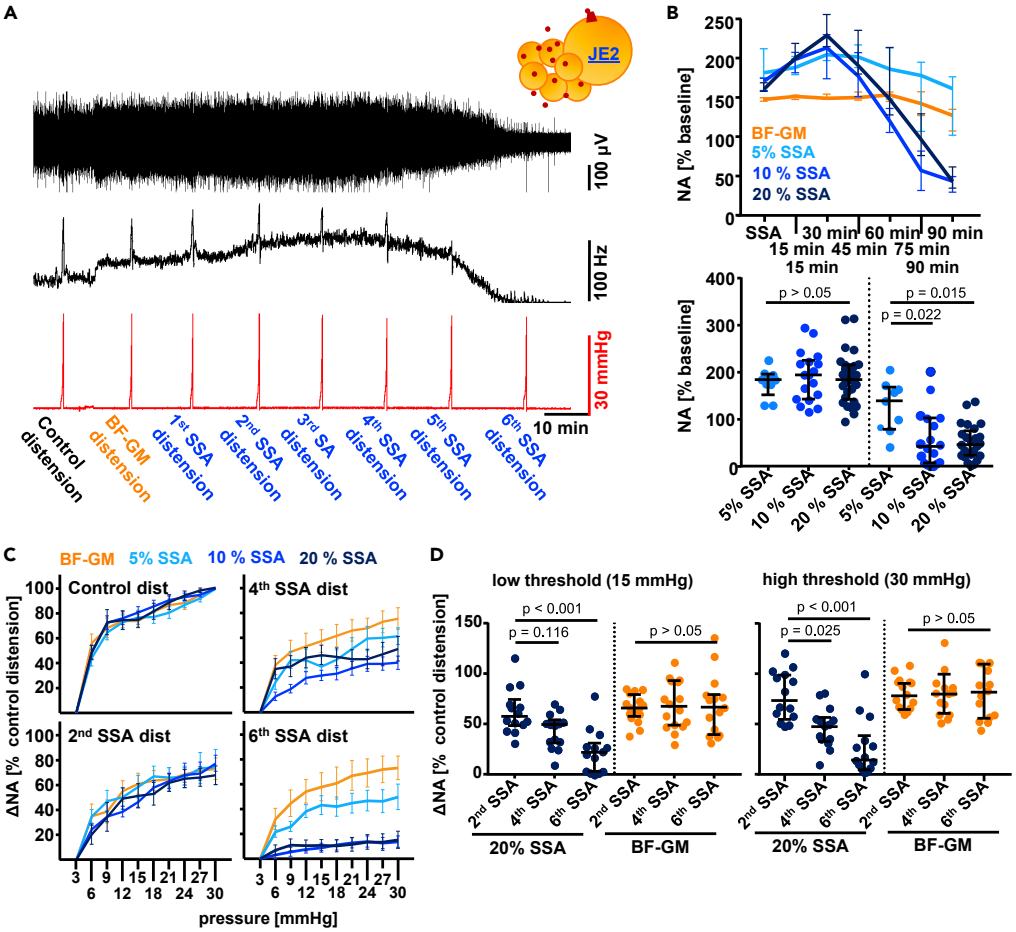

Figure 1. Bath Application of Supernatants from *S. aureus* (SSA) Strain JE2 Modulates Intestinal Sensory Nerve Activity (NA)

(A) Example trace of an experiment where 20% (v/v) SSA was applied for 90 min during which period the segment was distended every 15 min. Neurogram (top), firing frequency (mid), and intraluminal pressure (lower) were recorded throughout the experiment. Schematic in the top right corner indicates the usage of SSA-JE2 at high bacterial density. (B) The top panel shows the response profile of nerve activity during the application of different SSA concentrations or bacteria-free growth media (BF-GM). An initial increase of spontaneous discharge above BF-GM-induced changes was observed when 5%, 10%, or 20% (v/v) SSA were applied. Inhibition only occurred at higher concentrations. SSA-induced inhibition at 90 min but not excitation (15 min) was significantly different between 5% and 20% (v/v) SSA (lower panel). (C and D) SSA alter mechanosensitivity of small intestinal afferent nerves. (C) Distension-induced nerve activity decreased during prolonged (>45 min, fourth SSA distension) bath application of 10% or 20% (v/v) SSA. (D) Inhibition of both components of mechanosensitivity (LT, low threshold; HT, high threshold) contributed to the reduction of the distension response at late time points (distension 7, 90-min application), whereas only the HT component was significantly reduced at earlier time points. Data are median ± interquartile range. Non-parametric tests (Kruskal-Wallis test with Dunn's post-hoc analysis or two-sided Mann-Whitney test) were performed on data from N mice. N (5% SSA) = 11, N (10% SSA) = 18, N (20% SSA) = 14, N (BF-GM) = 16.

comparing the response to luminal distension before and during application of SSA. Under control conditions, we observed a 3.1-fold (median) increase of nerve activity in response to a control distension of 30 mmHg (Figure 1A). During SSA application (20% v/v), mechanosensitivity was profoundly inhibited, and in fact, sensitivity to distension was almost completely attenuated 75 min after SSA application (Figure 1C). This reduction of mechanosensitivity was concentration dependent and was not observed during vehicle application (Figures 1C and 1D). When we analyzed the change of nerve activity at 15 and 30 mmHg separately to investigate the low-threshold and high-threshold components, we found that both were reduced (Figure 1D), suggesting that SSA does not target distinct subpopulations of mechanosensitive fibers.

Heat-Labile QS-Regulated Mediators Excite and Inhibit Afferent Nerve Activity

SSA had a profound effect on spontaneous firing and mechanosensitivity of small intestinal afferents. We hypothesized that SSA contain soluble factors that exert a direct influence on afferent signaling from the GI tract and designed subsequent experiments to identify the nature of these mediators.

In experiments with SSA that were heated to 90°C for 15 min before bath application, the excitatory and inhibitory effects of SSA on spontaneous intestinal afferent firing were significantly attenuated (Figure 2A). AUC of the excitatory and inhibitory effects of SSA were determined as per Figure S2. Heat-treated SSA continued to inhibit mechanosensitivity, but to a lesser extent than the untreated SSA (Figure 2B). This indicates that both heat-stable and heat-labile mediators contribute to the effect of SSA on intestinal afferent firing with the latter having a predominant effect on spontaneous afferent firing and the former also influencing mechanosensitivity.

Environmental cues significantly affect SSA composition with population density being particularly important for determining the pattern of mediator expression (Chapman et al., 2017). The S-shaped OD_{600}-time relationship represents log, exponential, and stationary phases of bacterial growth (Figure S1C). SSA taken after various incubation periods excited afferent firing (Figure 2C). This was most pronounced with SSAs from 24-h cultures (with high optical density [OD]). The magnitude of inhibition increased progressively with increasing culture time (Figure 2D) and OD (Figure S1B). This suggests that it is *S. aureus* mediators released during the stationary growth phase (high OD) that exert a profound dual influence on intestinal afferent firing. Because high density activates QS mechanisms in bacteria, which increases the expression of exoproteins, our data are consistent with secreted proteins influencing afferent excitability.

In *S. aureus*, it is the accessory gene regulator (agr) system including the transcription factor AgrA that is particularly important for the QS-associated changes of protein expression. To confirm the importance of QS, we took a genetic approach and prepared SSA from an *S. aureus* JE2 mutant with a dysfunctional AgrA gene (SAUSA_1992; Centre for Staphylococcal Research, Nebraska library). Remarkably, SSA-$AgrA^-$ (20% v/v) had no effect on spontaneous afferent firing, nor did it affect either the low-threshold or high-threshold component of the mechanosensitive response to distension (Figures 2E and 2F). This complete dependence on AgrA is consistent with the finding that stationary phase mediators are necessary for any modulation of afferent firing.

Distinct Mediators Excite or Inhibit Afferent Activity

The transcription factor AgrA regulates the expression of genes that contribute to the pathogenesis of *S. aureus* such as PFTs and bacterial enzymes (LaSarre and Federle, 2013). The Nebraska library comprises JE2 mutants with dysfunctional genes encoding individual factors (Fey et al., 2013) and thus allows the study of their contribution to disease or in our case afferent sensitivity. In a candidate approach, we initially focused on heat-labile components because of our findings using heat-treated SSA.

α-Hemolysin (Hla) Contributes to Initial Increase of Nerve Activity

The JE2 wild-type strain produces large quantities of the PFTs Hla and Panton-Valentine leucocidin (Pvl). Both have been shown to increase intracellular calcium in sensory neurons and human neutrophils, respectively (Labandeira-Rey et al., 2007; Chiu et al., 2013; Cardot-Martin et al., 2015), and thus were chosen as a prime candidate for direct effects of SSA on intestinal afferent nerves. SSA prepared from the Hla-deficient JE2 mutant (SAUSA300_1058, SSA-Hla^-) did not induce the initial increase of nerve activity (Figure 3A left). The excitatory effect of SSA-Hla^- was significantly attenuated compared with wild-type SSA-JE2 (Figure 3A, middle). Similarly, the excitatory effect of SSA from the Pvl-deficient mutant (SAUSA300_1382, SSA-Pvl^-) appeared to be smaller than the overall excitatory effect induced by SSA-JE2 (Figure 3A middle), but the difference was not statistically significant. Both SSA-Hla^- and SSA-Pvl^- continued to inhibit spontaneous firing at later time points and also reduced mechanosensitivity of afferent firing (Figure 3A right, Figure 3B). These findings suggest that it is Hla that has direct effects on small intestinal nerve activity and is the predominant factor mediating the excitatory effect of SSA. Pvl plays a minor role, which may reflect the lower sensitivity of murine compared with human primary cells to this mediator (Spaan et al., 2017).

Phenol-Soluble Modulins Contribute to Inhibition of Spontaneous Firing and Mechanosensitivity

SSA lacking individual AgrA-regulated components (Hla, Pvl) continued to inhibit spontaneous firing and mechanosensitivity, which suggests that interaction of intestinal nerves with several mediators produced

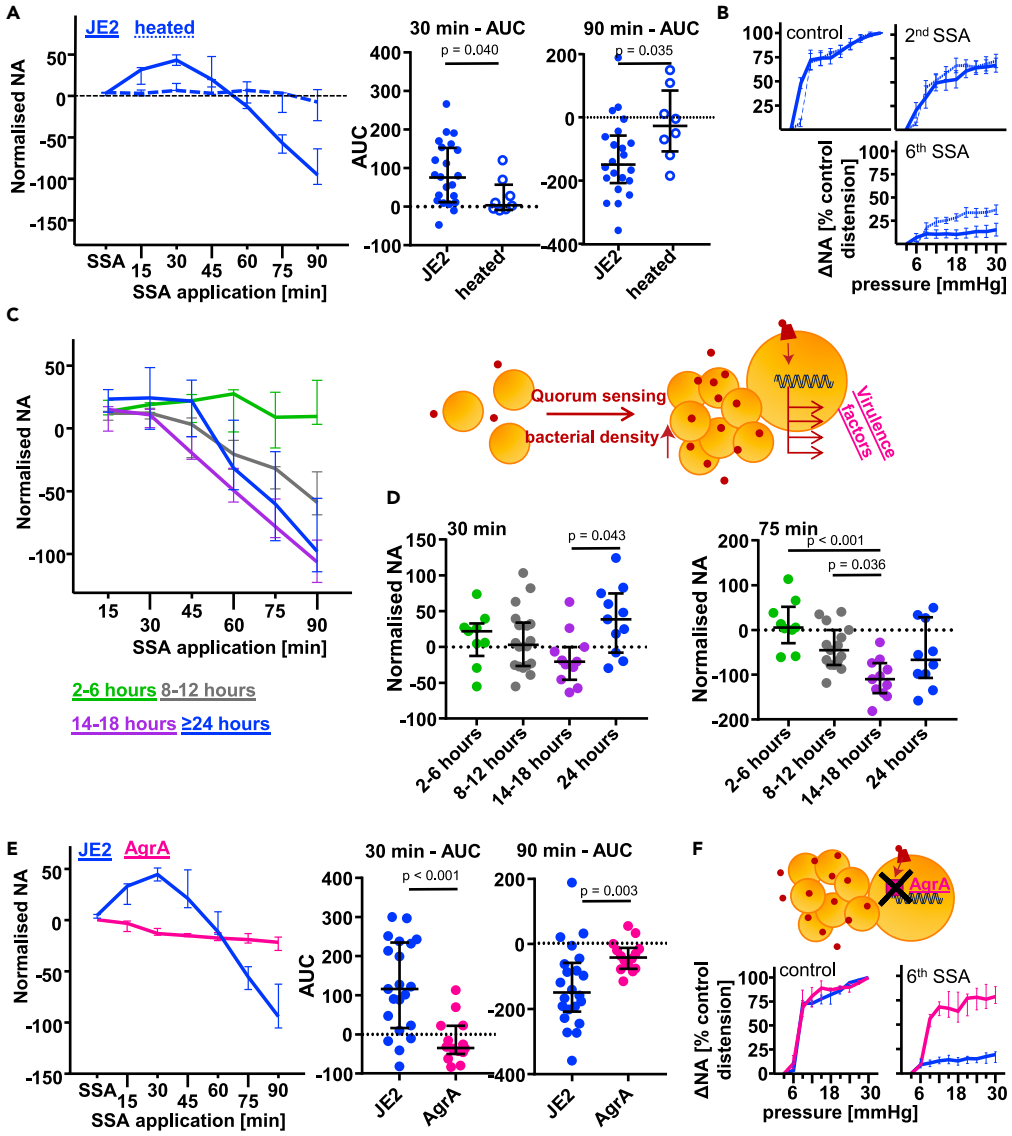

Figure 2. *S. Aureus* Produces Heat-Sensitive Soluble Mediators at Late Stages of Bacterial Growth that Modulate Small Intestinal Nerve Activity

(A and B) Heat treatment reduces the neuromodulatory effect of SSA. (A) Heating abolishes the effect of SSA on spontaneous discharge. Both excitatory (middle) and inhibitory (right) effects were significantly reduced. (B) Heat treatment does not entirely reverse the SSA-induced inhibition of mechanosensitivity.

(C and D) Bacteria were incubated for different periods and supernatants applied to small intestinal afferent nerves. (C) Response profile of afferent nerves during the bath application of 20% (v/v) SSA obtained after different incubation periods. (D) SSA obtained after 24 h of incubation had the largest effects on afferent NA. SSA from short-term cultures (<6 h) tended to increase nerve activity at 30 min (left) but did not reduce spontaneous firing at later time points (right). Schematic indicates the usage of supernatants from cultures with different bacterial density representing different stages of bacterial growth.

(E and F) The release of neuromodulatory substances in S. *aureus* is dependent on quorum sensing-activated gene regulation (schematic). (E) SSA from the quorum sensing mutant (agrA^{-}) had no effect on spontaneous discharge. In the absence of AgrA, excitation (middle panel) and inhibition (right panel) were significantly alleviated. (F) SSA-AgrA^{-} did not reduce mechanosensitivity. NA, nerve activity; AUC, area under the curve. Data are median ± interquartile range. Non-parametric tests (Kruskal-Wallis test with Dunn's post-hoc analysis or two-sided Mann-Whitney test) were performed on recordings from N mice. N(2-6) = 9, N(8-12) = 16, N(14-18) = 12, N(24) = 11, N (≥24) = 14, N(JE2) = 22, N(heat-treated) = 8, N(AgrA) = 14.

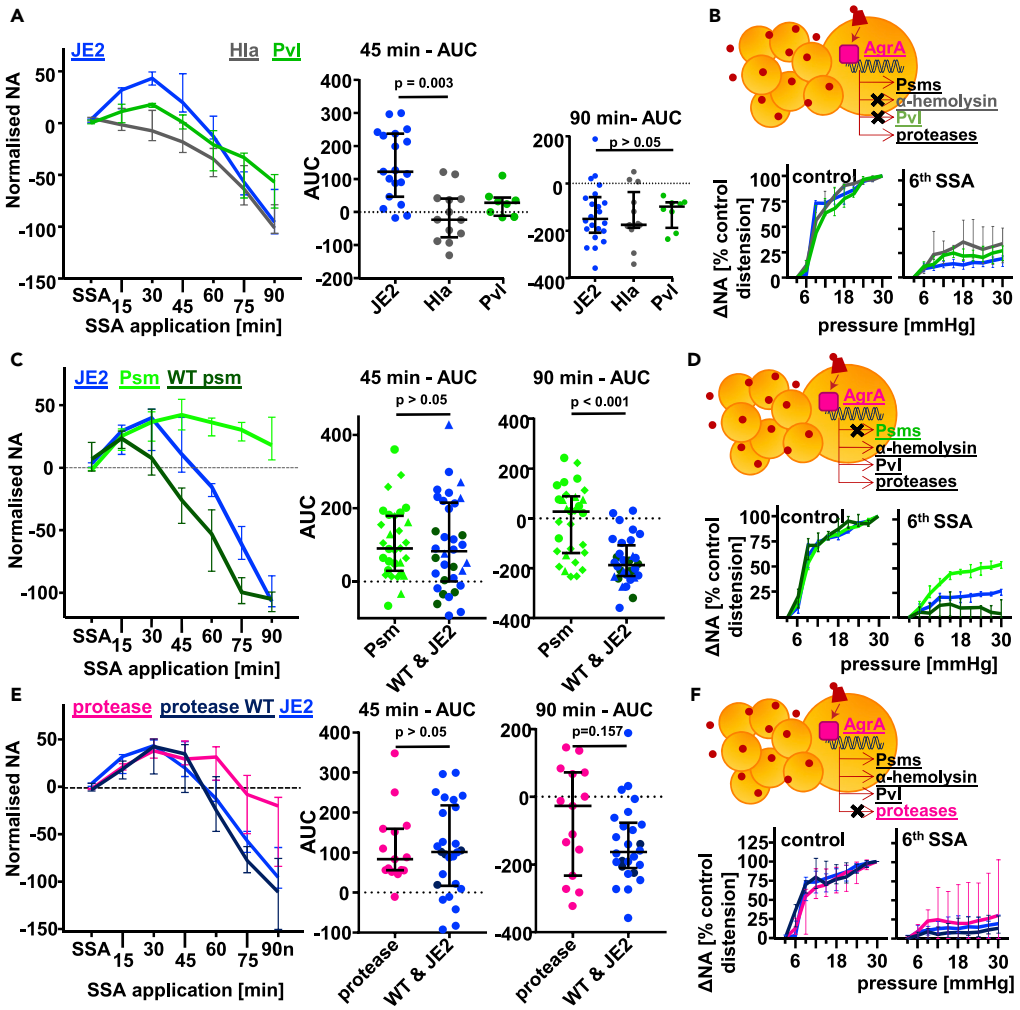

Figure 3. Investigation of the Contribution of Individual Soluble Mediators to the Excitatory and Inhibitory Effect of SSA

(A and B) Contribution of individual toxins to the neuromodulatory effects of SSA (schematic). (A) The absence of α-hemolysin (Hla) or Pantom-Valentine leucocidin (Pvl) decreases the excitatory component (middle panel), which was significant for Hla. The inhibitory component was not affected by a lack of Hla or Pvl (right panel). (B) Mechanosensitivity decreases during incubation with SSA from wild-type JE2 as well as its hla^{-} and pvl^{-} mutants.

(C and D) Phenol-soluble modulins (Psms) contribute to the inhibitory effects of SSA. (C) SSA lacking Psms continue to increase spontaneous discharge (left and middle panels). The inhibitory effect of SSA-JE2 was significantly reduced in the absence of Psms (right panel). Psm-deficient SSAs were used in three sets of experiments, which are represented by the shape of the data point. No inhibition (AUC >0) was observed in 9 of 11 (81.2%, circles), 7 of 17 (41.2%, diamonds) and 4 of 6 (66.7%, triangles). The response to the JE2-derived wild-type for the psm mutant (WT psm) was not significantly different from the JE2 used as a control in other experiments. (D) Mechanosensitivity was partially rescued when Psms were not present in SSA-JE2. N(Psm) = 34, N(Psm WT) = 8, N (JE2) = 41.

(E and F) Protease-deficient SSA continue to modulate small intestinal nerve activity. (E) Response profile of NA during application of SSA lacking bacterial proteases (left panel). Excitation was not alleviated (middle panel). Inhibition was not observed in some experiments with protease-deficient SSA, but the alleviation was not significant (right panel). The response to the JE-derived wild-type for the protease mutant (protease WT) was not significantly different from the JE2 used in previous experiments. (F) Protease-deficient SSA decreased mechanosensitivity similar to wild-type SSA. NA, nerve activity; AUC, area under the curve. Data are median ± interquartile range. Non-parametric tests (Kruskal-Wallis test with Dunn's post-hoc analysis or two-sided Mann-Whitney test) were performed on preparations from N mice. N(JE2) = 22, N(Hla) = 13, N(Pvl) = 8, N(protease) = 15, N(protease WT) = 4.

by S. *aureus* is involved in the complex effects of SSA. Nerve inhibition could be the result of alterations in membrane permeability, especially because the JE2 strain produces large quantities of amphipathic substances with a high affinity for lipids. Phenol-soluble modulins (Psms) constitute a group of seven short peptides with an α-helical structure (Wang et al., 2007) that can insert into liquid-disordered membrane domains. A mutant lacking the seven Psms is not available in the Nebraska library but has been generated, validated, and generously provided by Michael Otto (NIH).

SSA from this mutant (SSA-Ps$^-$) excited small intestinal sensory nerves to a degree, which was similar to the wild-type (Figure 3C). With regard to inhibition, we observed a particularly large variability of the responses to SSA from this mutant (Figure 3C). Overall, however, the inhibitory effect of SSA was significantly reduced by the lack of Psms (Figure 3D). This suggests that Psms contribute to inhibition of spontaneous nerve firing, at least in most animals. In others, additional factors also contribute to the inhibitory effect of SSA. To verify the predominant role of Psm in inhibiting nerve activity, we recorded from nerves innervating the proximal colon where bacterial density is higher than in the small intestine. In agreement with our findings in the small intestine, SSA-JE2 caused a similar biphasic response pattern consisting of an excitatory and inhibitory phase, although the degree of excitation was smaller and the onset of inhibition occurred earlier. This profound inhibition of colonic afferents was absent in 80% of experiments using Psm-deficient SSA (Figure S4). With regard to targeting subpopulations of mechanosensitive afferent fibers, we found that there was a selective effect of Psms on low-threshold fibers (Figure S3B). Those continued to fire at higher rates when SSA lacking Psms were applied compared with SSA-JE2. At later time points, however, both low- and high-threshold components of the response were significantly higher during SSA-Psm$^-$ compared with SSA-JE2 application (Figure S3C), which indicates that Psms reduce the distention-induced firing across a range of mechanosensitive populations.

Bacterial Proteases Have a Limited Role in the Effects of SSA on Afferent Nerve Activity

In addition to exotoxins, AgrA regulates the expression of bacterial proteases. These are essential for tissue invasion during pathogenesis, and proteases have previously been shown to modulate intestinal sensory signaling (Adams et al., 2011; Delmas et al., 2011).

We obtained a JE2 mutant missing 10 of S. *aureus*'s major proteases (Kolar et al., 2013), which include cysteine and metallo- and serine proteases. In the intestine, serine proteases have been shown previously to activate sensory neurons (Buhner et al., 2018). SSA from the protease-deficient mutant (SSA-Prot$^-$) evoked a biphasic effect on spontaneous afferent firing similar to that seen with wild-type SSA. The onset of inhibition tended to be delayed and the degree of inhibition attenuated (Figure 3E), although not significantly. The profound attenuation of mechanosensitivity induced by SSA-JE2 persisted with SSA-Prot$^-$ (Figure 3F). Overall, this suggests that *S. aureus*'s proteases do not play a major role in SSA-mediated neuromodulation, and if anything may contribute to inhibition rather than excitation as seen in previous studies (Cenac, 2013).

SSA-Mediated Changes of Membrane Permeability

We identified PFTs as major neuromodulatory molecules in SSA. Therefore, we quantified SSA-induced changes of membrane permeability using propidium iodide (PI) fluorescence in primary cultures of sensory neurons. SSA caused a marked increase in PI fluorescence (Figures 4A and 4B). This effect was concentration dependent, and at 5% and 10% v/v dilution, the majority of cells responded (Figure 4C left). The average response latency was also concentration dependent and decreased dose dependently (Figure 4C right). An increase of the concentration above 1% v/v had no further impact on the δfluorescence per coverslip as a measure of overall responsiveness. Higher concentrations decreased the variability of the response latency, which was high at low concentrations (Figure 4C right).

Our next aim was to establish which components in SSA mediated the increase of PI fluorescence and thus applied SSA from different S. *aureus* mutants. At a concentration of 10%, SSA-AgrA$^-$ and SSA-Psm$^-$ did not increase PI fluorescence (Figure 4B) indicating that AgrA regulates the production of components that change membrane permeability with a major role for Psms. At a concentration of 10% SSA, the lack of Hla (SSA-Hla$^-$) did not significantly affect the response pattern (Figure 4D right) or the δfluorescence per coverslip compared with SSA-JE2 (not shown). There were, however, significant differences in the number of responding cells and their response latency between SSA-Hla$^-$ and SSA-JE2 (Figure 4D, left) at a

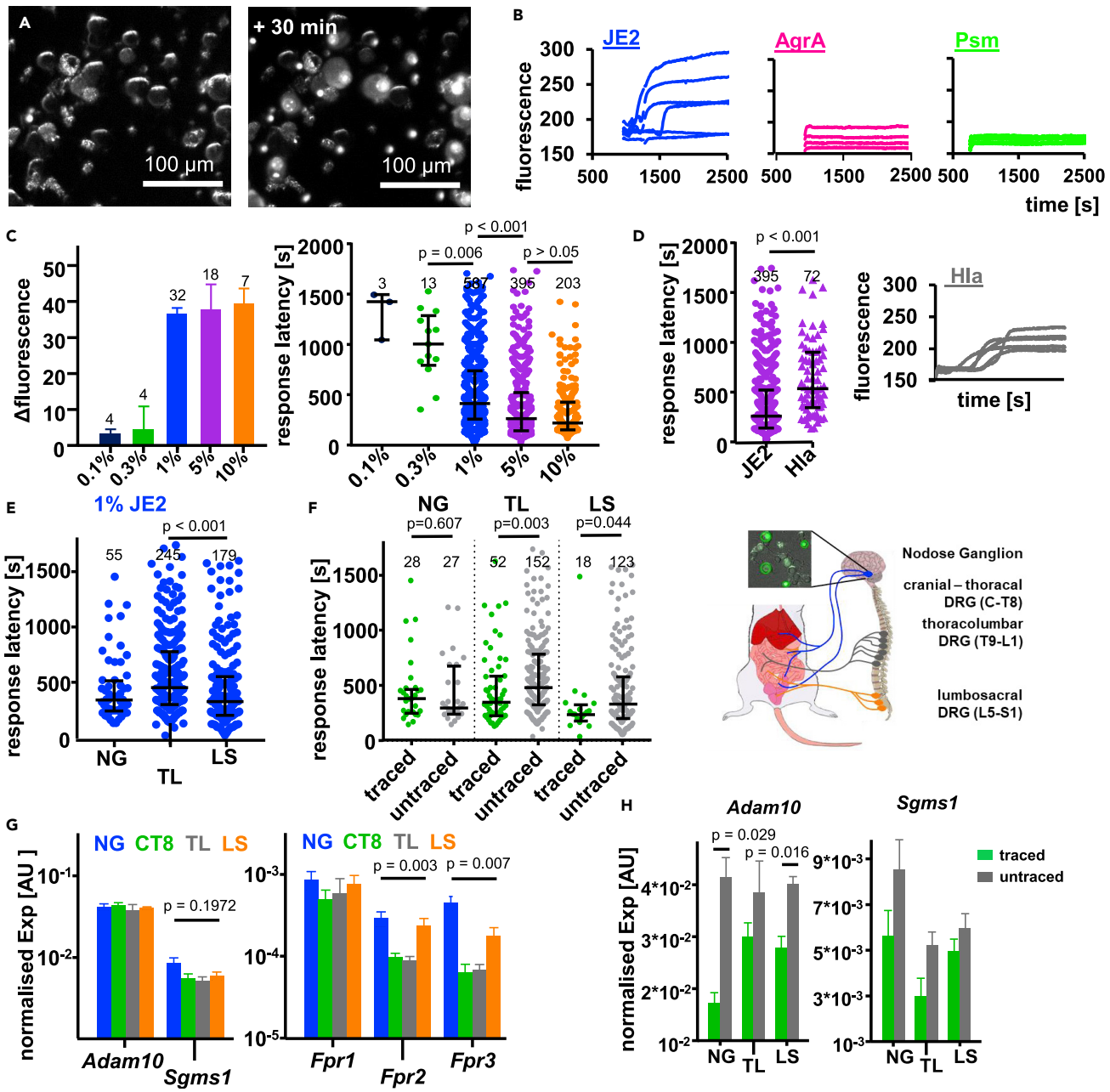

Figure 4. Effect of Soluble Mediators from SSA on Cell Membrane Permeability

(A and B) Dorsal root ganglia (DRG) neurons were isolated and incubated with propidium iodide (PI). PI fluorescence was recorded during application of SSA. (A) Example images before (left) and after (right) application of SSA. (B) SSA (10% v/v) from *S. aureus* JE2 but not the AgrA or Psm-deficient mutants increase PI fluorescence.

(C) The change of fluorescence (left) per coverslip as a measure for the number of responding cells increases concentration dependently. In contrast, the response latency (right) of responding cells decreases.

(D) SSA lacking Hla continue to increase PI fluorescence (right), but at a concentration of 5% v/v, the response latency was significantly longer compared with wild-type SSA-JE2.

(E–H) Spinal localization and peripheral projection affect the response latency to 1% (v/v) SSA-JE2. The mRNA expression (Exp) of putative receptors for Hla and Psm was investigated in these subpopulations. (E) Thoracolumbar (TL) DRG had longer response latencies than lumbosacral (LS) DRG and nodose ganglia (NG): median(LS) = 237.1 s, median(TL) = 355 s, median(NG) = 280 s. (F) Neurons that project to the viscera were identified by intraperitoneal injection of the green fluorescent tracer CTB-488 (schematic on the right; constitutes a composite from http://ctrgenpath.net/static/atlas/mousehistology/Windows/digestive/mousediagram.html and Sanders et al., 2012: Regulation of gastrointestinal motility-insights from smooth muscle biology). Visceral neurons from TL and LS DRG had shorter response latencies. (G) DRG express mRNA for *Adam10*, *Sgms1*, and formyl peptide receptors (*Fprs*); p values for

Figure 4. *Continued*

Kruskal-Wallis test per gene. (H) Receptors for Hla were expressed in isolated visceral neurons at all levels of the spinal cord. *Fpr* expression was below the detection limit in these experiments.

AU, arbitrary unit. Data are median ± interquartile range (C, D, E, and F) or mean ± SEM (G and H). Non-parametric statistical analysis (Kruskal-Wallis test with Dunn's post-hoc analysis or two-sided Mann-Whitney test) was performed; n numbers as indicated (coverslips in or cells) obtained from N = 4–5 animals.

concentration of 5% v/v, indicating that Hla also contributes to SSA-induced changes of membrane permeability.

We hypothesized that the variability of response latencies reflected heterogeneity in dorsal root ganglia (DRG) neuronal subtypes and their visceral targets. We therefore compared response latencies between sensory neurons from the nodose ganglion (NG), thoracolumbar (TL), and lumbosacral (LS) DRG. TL neurons had significantly higher response latencies than LS neurons (Figure 4E). They also tended to respond later than NG neurons, although this was not significant (Figure 4E). We identified abdominal visceral neurons through intraperitoneal injection of the fluorescent tracer CTB-488 (Peeters et al., 2006) and compared response latencies between labeled and unlabeled neurons. Traced LS neurons were more susceptible to SSA compared with traced neurons from other sensory ganglia. Labeled LS and TL neurons had significantly shorter response latencies than unlabeled neurons, whereas the response latencies of traced and untraced neurons in the NG were not statistically different (Figure 4F). This suggests that viscera-projecting DRG neurons have greater susceptibility to SSA.

We next analyzed the mRNA expression of the putative receptors for Psms and Hla in these neuronal populations (Figures 4G and 4H). These include formyl peptide receptors (FPRs), a disintergrin and metalloprotease 10 (ADAM10), and sphingosine, which is synthesized by sphingomyelin synthase 1 (SGMS-1) (Inoshima et al., 2011; Schreiner et al., 2013; Virreira Winter et al., 2016). The expression of *Fpr2* and *Fpr3* was higher in NG and LS neurons compared with TL neurons, whereas *Adam10* and *Sgms1* were more uniformly expressed (Figure 4G). This indicates that afferents projecting via pelvic and nodose pathways are more susceptible to SSA and express higher amounts of the Psm receptors *Fpr2* and *Fpr3* than splanchnic afferents from TL DRG. For comparison, we also examined expression in intestinal tissue and found across the board a lower level of expression in the gut wall compared with DRG (Figure 5A).

Modulation of Epithelial Secretion and Motility

In a final series of experiments, we sought to determine the functional consequence of SSA on intestinal secretion and motility, which are in part regulated by intrinsic intestinal neurons. Serosal application of 10% v/v SSA-JE2 induced a profound increase of short circuit currents (SCC), reflecting electrolyte secretion, which was characterized by an initial steep increase that plateaued after approximately 10 min (Figure 5B). At lower concentrations (1%,Figure S5), the overall increase (AUC) as well as the slope of the early response was significantly smaller than at 10% SSA-JE2. SSA from the different mutants had a differential effect on SCC. A significant reduction in AUC and initial slope was observed with the QS mutant (SSA-AgrA$^-$). SSA lacking either Hla or Psm also had a smaller prosecretory effect than SSA-JE2, but this difference was only significant for SSA-Hla$^-$ (Figure 5C), which indicates that Hla plays a major role SSA-induced secretion.

Distension-induced colonic motility consists of motor complexes with large amplitude contractions interspersed by periods of quiescence (Figure 5D). Bath-applied SSA-JE2 (5%) significantly reduced contraction amplitude compared with the BF-GM vehicle (Figure 5E, top). This inhibitory effect was not observed when SSA were prepared from the JE2 QS mutant (SSA-AgrA$^-$), further highlighting the profound effect of QS-regulated virulence factors on intestinal function. In sharp contrast to the reduction of contraction amplitude, frequency of contractions was unaffected by *SSA* (Figure 5E, bottom).

DISCUSSION

In the present study, we have used a genetic approach to demonstrate a role of bacterial QS-regulated genes in bacteria-gut-brain communication. Two classes of heat-labile membrane-interacting toxins, Hla and phenol-soluble modulins, were found to contribute to excitation and inhibition of small intestinal and colonic afferent firing. Hla and phenol-soluble modulins also modulate epithelial secretion and motility.

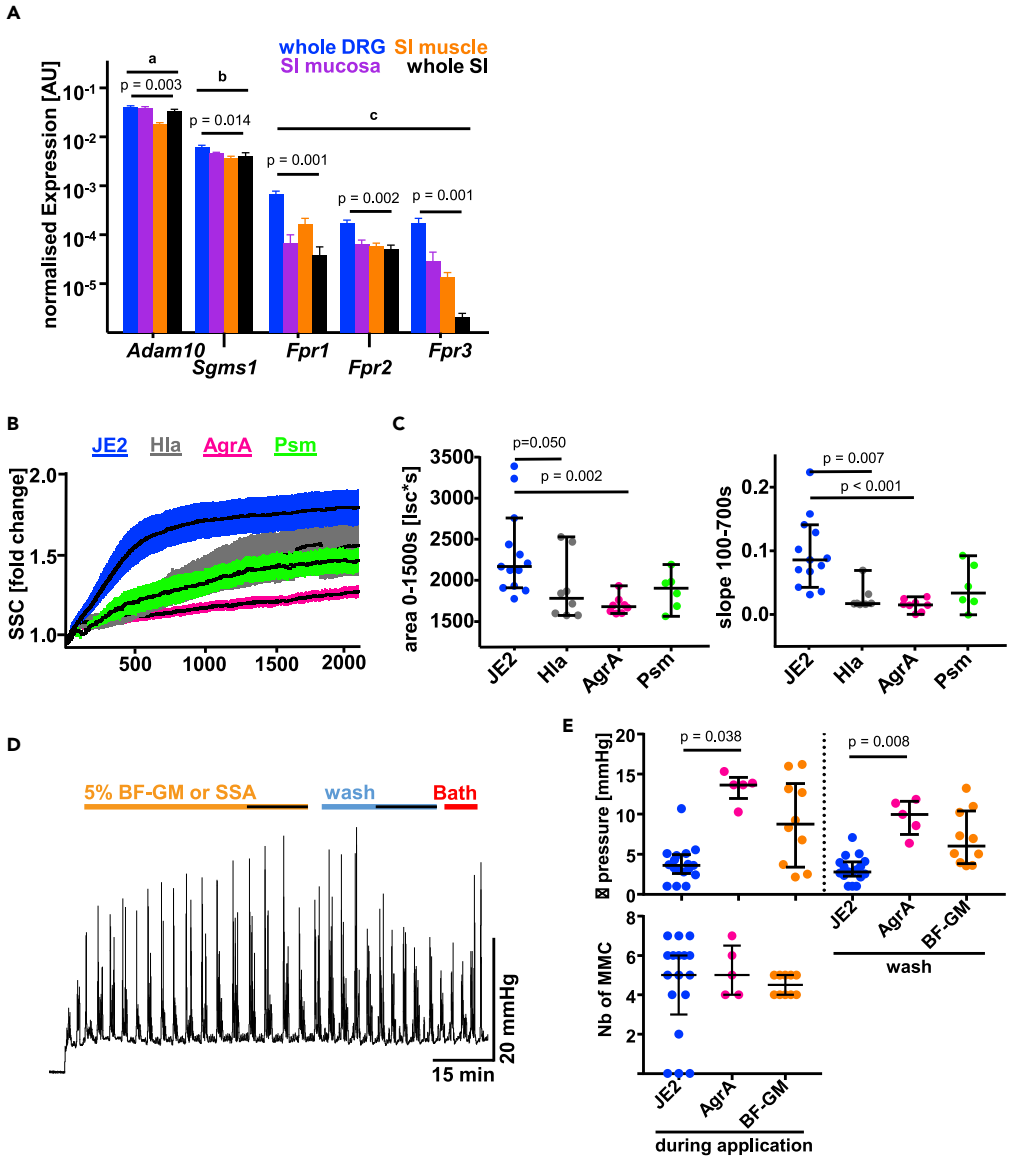

Figure 5. Soluble Mediators in SSA-JE2 Affect Intestinal Function

(A) mRNA for *Adam10*, *Sgms1*, and *Fprs* is expressed in intestinal tissue. The expression level is lower than in dorsal root ganglia (p values). The abundance *Fpr* mRNA was lower than those of *Sgms1* mRNA and *Adam10* mRNA (letters). AU, arbitrary unit. Data are mean ± SEM (N = 4–5 mice). For whole DRG, data from Figure 4F excluding NG were averaged; p values for Kruskal-Wallis test per gene.

(B and C) SSA (10% v/v) were applied to mucosa-submucosa preparations from mouse small intestine in Ussing chambers and short circuit currents (SCC) were recorded. (B) Aligned overlay of SCC measurements (mean ± SEM) for different *S. aureus* mutants. (C) The SSA-induced increase of AUC was significantly smaller in the AgrA mutant compared with wild-type JE2 (left). The slope of SSA-induced increase SCC was smaller when AgrA-as well as Hla-deficient supernatants were applied. Data are median ± interquartile range N (JE2) = 13, N(Hla) = 8, N(AgrA) = 8, N(Psm) = 6 from seven animals.

(D and E) SSA (5% v/v) were bath applied and colonic contractions induced by distension. (D) Example trace for motility recordings where SSA were applied for 60 min directly after inducing migrating motor complexes (MMC) in the colon followed by a 30-min washout period. Contraction amplitude and number were determined in the 15-min interval at the end of the incubation period. (E) SSA-JE2 decreased contraction amplitude, which was reverted when the quorum sensing regulator AgrA was mutated (top panel). The number of MMC (bottom panel) was not statistically different between SSA-JE2, SSA-AgrA$^-$, and bacteria-free growth medium (BF-GM). Data are median ± interquartile range. N(AgrA) = 5; N(BF-GM) = 8, and N(JE2) = 17 preparations. One preparation per mouse.

Non-parametric statistical analysis (Kruskal-Wallis test with Dunn's post-hoc analysis or two-sided Mann-Whitney test) was performed.

Bacteriological Approach to Investigate Host-Pathogen Interaction

To study a direct interaction between bacterial mediators and neurons, we used supernatants of bacterial cultures with well-described genotypes containing a number of secreted virulence factors. Previous studies have applied supernatants from mucosal biopsies or fecal samples to isolated neurons and intestinal nerves to investigate mechanisms underlying changes of visceral sensitivity (Ibeakanma et al., 2011; Valdez-Morales et al., 2013; Sessenwein et al., 2017) and have identified a role for both host and bacteria-derived mediators, respectively (Ibeakanma and Vanner, 2010; Valdez-Morales et al., 2013). Others have used individual mediators in a more targeted approach to provide a more mechanistic analysis (Ochoa-Cortes et al., 2010; Dinic et al., 2018). In this study, we demonstrated that selective genetic modification of bacteria in combination with electrophysiological recordings is a powerful tool to "dissect out" the contribution of individual mediators in modulating intestinal sensory function.

Pathways Contributing to Bacteria-Neuron Communication

Our study provides evidence for a direct interaction between exotoxins secreted by *S. aureus* and intestinal neurons. Previously, neuronal activation in response to microbes has been attributed to the bacterial release of neurotransmitters (Pokusaeva et al., 2017; Bhattarai et al., 2018; Strandwitz et al., 2019), bacterial cell-wall components, or metabolites. Cell-wall components either directly activate neurons (Mao et al., 2013) or induce the release of neuropeptides, ATP, or cytokines from epithelial or immune cells (Gourbeyre et al., 2015). Bacterial metabolites such as short-chain fatty acids, tryptophan metabolites, and trace amines can activate neurons through a plethora of receptors (Korecka et al., 2016; Cohen et al., 2017; Obata et al., 2020). Our study adds exotoxins regulated by QS to this growing list of bacterial neuromodulatory mediators.

Our data are consistent with a direct effect of bacterial mediators on sensory signaling. However, there is potential for enterochromaffin (EC) cells and resident immune cells, particularly mast cells, to be intermediaries in the signaling pathway. Indeed, mast cells are implicated in the diarrhea triggered by *S. aureus* peptidoglycan (Feng et al., 2007), but this is unlikely to contribute to the heat-labile effects observed here. Certainly mast cell mediators including 5-hydroxytryptamine, histamine, and mast cell tryptase in supernatant from patients with irritable bowel syndrome can exert an excitatory influence on both extrinsic afferents (Cenac et al., 2007; Song et al., 2015) and intrinsic submucosal neurons (Buhner et al., 2009, 2018). Moreover, mast cells are in close proximity to sensory nerve endings, and thus degranulation products will have ready access to these nerve endings (Gupta and Harvima, 2018). However, these mast cell effects are generally excitatory, whereas inhibition of afferent firing was a predominant finding in these studies. In addition, the effects on peripheral afferent firing were mirrored in the DRG preparations devoid of EC cells and mast cells. Our finding that intestinal neurons express putative receptors for these mediators further supports this novel concept by which bacteria may alter intestinal function and gut-brain communication.

Phenol-Soluble Modulins (Psms)

Our experiments using supernatants from a mutant *S. aureus* lacking Psms (SSA-Psm^{-}) suggest a major role of Psms in bacteria-induced modulation of gut-brain axis. The inhibition of spontaneous and distension-evoked afferent firing induced by wild-type SSA as well as SSA-induced membrane permeabilization of DRG neurons was markedly attenuated using Psm-deficient SSA. Psms are a group of short amphipathic peptides highly expressed by pathogenic *S. aureus* (Wang et al., 2007) and have been shown to effectively lyse human neutrophils, erythrocytes, and T cells (Wang et al., 2007; Laabei et al., 2014). Others have found that Psm-α3 induces calcium transients and action potential firing in cultured neurons (Blake et al., 2018), which might imply an excitatory rather than inhibitory effect. Psms have also been shown to increase intracellular calcium via interaction with the formyl peptide receptor (Rautenberg et al., 2011), again consistent with an excitatory effect. We and others have found that *Fprs* are expressed in sensory ganglia and they were also detected in some colon-innervating DRG neurons (Hockley et al., 2018). It is possible that the excitatory effect leads to a longer-term excitotoxicity and inhibition of firing. However, as in our study excitation persists in the absence of inhibition, these would appear not to be linked. In contrast, it may be that receptors other than Fprs are involved in Psm-mediated nerve inhibition. Their structural similarity to β-defensins and other ligands of the human mas-related G-protein-coupled receptor MRGPRX2 (Bader et al., 2014) suggests that MRGPRs are involved in Psm-mediated effects (Nakamura et al., 2013). Functional Mrgprs have recently been implicated in visceral hypersensitivity. Ligands for Mrgpra1, Mrgprc11, and Mrgpd excited colonic afferents and isolated DRG neurons (Bautzova et al., 2018; Castro et al., 2019), which

suggest that Psms activate different mechanisms because they inhibited sensory afferents. Psms can also change the properties of the cell membrane (Laabei et al., 2014). This has recently been shown to be the mechanism by which QS metabolites produced by *Pseudomonas aeruginosa* activate an immune response (Song et al., 2018).

α-Hemolysin (Hla)

In contrast to the prominent role of Psms in inhibition, we found that Hla contributes to excitation of intestinal afferents. Thus, SSA from the Hla mutant of *S. aureus* caused a monophasic inhibition. These observations are consistent with previous studies showing that Hla can induce action potential firing and calcium transients in primary sensory neurons (Chiu et al., 2013). Our observation that Hla-deficient SSA continued to increase PI in DRG neurons also suggests that it is ion influx through pores formed by Hla that directly increases neuronal excitability. Given its pore-forming capacity, it is intriguing that Hla, in contrast to Psms, did not contribute to inhibition of intestinal nerve activity. This might indicate that Hla-induced pores are less disruptive for the cell membrane. Indeed, Hla pores have a defined structure that allows the passage of ions (Ca^{2+}, K^{+}) and nucleotides (Menestrina, 1986; Vandenesch et al., 2012). Our finding that *Adam10* is expressed in sensory neurons suggests a possible mechanism of action of Hla. *Adam10* is a membrane-bound metalloprotease that is implicated in Hla pore formation. *Adam10* is required for Hla binding and also needed for Hla-mediated cytotoxicity (Wilke and Wardenburg, 2010).

In addition to Hla, other PFTs such as Pvl could also contribute to the excitation caused by SSA. We found that Pvl-deficient SSA tended to induce attenuated excitation compared with wild-type SSA (SSA-JE2). Blake et al. (2018) reported that the two-component leucocidin HlgAB can activate DRG neurons contributing to pain signaling (Blake et al., 2018). Our data suggest that multiple mechanisms contribute to pore formation and may have redundant and synergistic functions (Los et al., 2013). In both this and the previous studies, however, it was Hla that played the major role in increased intestinal afferent firing and spontaneous pain during *S. aureus* infection, respectively, which may imply that the large excitatory response in our study directly reflects a nociceptive signal.

Proteases

Recent studies have shown an inhibitory effect of commensal strains of bacteria on DRG excitability, which was mediated by serine proteases acting on PAR4 receptors (Sessenwein et al., 2017) and may contribute to their pain regulating effects. In our microbiological approach, we used strains of *S. aureus* devoid of bacterial proteases to investigate protease involvement in intestinal afferent signaling. We found that SSA from these bacteria continued to generate a biphasic afferent response with excitation followed by inhibition. The inhibitory effect was attenuated, but this was not significantly different from wild-type. However, in about half of the experiments the inhibitory effect was absent using the protease mutant. This variability is inherent in studies of bacteria-host interaction because of the marked effect of population density and environmental factors in the secretion of virulence factors (Blake et al., 2018). Thus, bacterial proteases may not directly contribute to sensory signaling. However, because bacterial proteases are important virulence factors for tissue invasion it is possible that, *in vivo*, they facilitate the penetration of neuromodulatory components to nerve terminals situated beneath the mucosal epithelium.

Functional Relevance

We have identified a novel communication pathway between bacteria and intestinal neurons utilizing exosecreted mediators. *In vivo* these and other mediators will activate the host's immune system, which will also contribute to neural signaling following release of a variety of inflammatory mediators. The relative extent to which direct and indirect mechanisms contribute to the overall neural response must await *in vivo* studies but is likely to vary depending on the extent and stage of infection. Indeed, an *in vivo* investigation of somatic pain assessed using the limb withdrawal reflex observed an initial period of hypersensitivity that mirrored the bacterial load followed by a later phase associated with recruitment of an inflammatory response (Chiu et al., 2013). In the GI tract, these bacterial mediators have the potential to directly influence intestinal symptoms and reflex function *in vivo*, and together with immune-mediated changes of neuronal activity may contribute to homeostatic, behavioral, and sensory consequences of infection.

It was notable that viscera-projecting DRG neurons had a greater susceptibility to SSA than those that innervate other tissues. Afferents projecting via the nodose and pelvic pathways were also more susceptible to SSA and expressed higher amounts of the Psm receptors *Fpr2* and *Fpr3* than splanchnic afferents.

This is important as these pathways innervate the respective oral and aboral ends of the GI tract, suggesting that these visceral neurons act as "sentinels" to notify us of the consumption, and induce the expulsion of opportunistic pathogens. This potentially provides an evolutionary mechanism to reduce the harmful effects of pathogen ingestion.

Accordingly, bacterial mediators may also induce important reflex functions including altered secretion, motility, and neuro-immune interactions, by interacting with other targets within the gut wall such as enteric neurones, smooth muscle cells, and epithelium. In terms of secretion, SSA-JE2 caused a profound increase of transepithelial ion movements as revealed by changes in short-circuit current. Like the neuromodulatory effects described above, this was dependent on QS-regulated molecules because the response was attenuated in the AgrA mutant. It was the Hla-deficient SSA that exerted the most significant attenuation of SSA-induced secretion. Hla has been shown to induce epithelial damage via *Adam10*-mediated cleavage of cell-adhesion proteins such as E-cadherin (von Hoven et al., 2016). Virulence factors in SSA-JE2 were also found to modulate colonic contractile activity. Wild-type SSA caused a reduction of the amplitude of colonic motor complexes. This again was lost using SSA from the QS mutant. AgrA-regulated molecules have been shown to be important for intestinal colonization of *S. aureus* (Piewngam et al., 2018). Interestingly, commensal and probiotic bacteria can also inhibit contractions (Massi et al., 2006; Guarino et al., 2008; Gong et al., 2017), but this is mediated by cell-wall glycolipids (Mao et al., 2013).

In conclusion, our findings constitute a paradigm shift in our thinking about the microbiota-gut-brain axis. In contrast to previous views in which the focus is on immune activation, we suggest that a direct interaction between intestinal neurons and QS-regulated bacterial mediators is involved in sensory signaling during bacterial infections. Additionally, interaction of these components with intrinsic intestinal neurons and epithelial and smooth muscle cells may underlie symptoms such as diarrhea and dysmotility. The dependence on growth phase mediators and QS mechanism reflects the complex interplay between bacteria and their host.

Limitations of the Study

In this study we confirmed that neurons contribute to intestinal bacterial sensing and microbiota-gut-brain axis through direct interaction with soluble molecules released by bacteria. Although using an *in vitro* approach provided a unique opportunity to intricately dissect these mechanisms in isolation, independent of the host immune system, *in vivo* there is scope for bacteria to interact directly with the immune system, which may provide secondary modulation of neuronal excitability. We used a novel genetic approach using supernatants from cultures of *S. aureus* to identify potential neuromodulators (Hla, phenol-soluble modulins) that are likely to directly influence intestinal symptoms and reflex function *in vivo*. Whether such mediators contribute to common symptoms associated with pathophysiological conditions of the GI tract is yet to be determined and will be an exciting area for future research.

Resource Availability

Lead Contact

Further information and requests for resources and reagents should be directed to and will be fulfilled by the lead contact, Prof David Grundy, d.grundy@sheffield.ac.uk.

Materials Availability

This study did not generate new unique reagents.

Data and Code Availability

The original unprocessed data of live cell imaging and electrophysiological recordings are contained in very large files that can only be read with specialist software. These are available from the corresponding authors upon request. All raw data are available upon reasonable request and will be provided in a timely manner.

METHODS

All methods can be found in the accompanying Transparent Methods supplemental file.

SUPPLEMENTAL INFORMATION

Supplemental Information can be found online at https://doi.org/10.1016/j.isci.2020.101695.

ACKNOWLEDGMENTS

The research leading to these results has received funding from the People Programme of the EU's Seventh Framework Programme under REA grant agreement no. 607652 (ITN NeuroGut). S.M.B is supported by a National Health and Medical Research Council of Australia (NHMRC) R.D Wright Biomedical Research Fellowship (APP1126378), and by National Health and Medical Research Council Australia Project Grants APP1140297 and APP1139366. The authors would like to thank D. Krueger and M. Schemann (TU Munich, Germany) for sharing their expertise in Ussing Chamber recordings and M. Otto (NIH) and A. Gründling (Imperial College London) for providing the psm- and protease-deficient S. *aureus* mutants.

AUTHOR CONTRIBUTIONS

Conceptualization: D.G., F.U., and S.J.F., Investigation: F.U., Methodology: L.G. and S.G.-C., Resources: D.G., S.J.F., and S.M.B., Supervision: D.G., Writing – Original Draft: D.G. and F.U., Writing – Review & Editing: D.G., F.U., L.G., S.G.-C., S.M.B., and S.J.F.

DECLARATION OF INTERESTS

The authors declare no competing interest.

Received: May 13, 2020
Revised: July 3, 2020
Accepted: October 14, 2020
Published: November 20, 2020

REFERENCES

Acton, D.S., Tempelmans Plat-Sinnige, M.J., Van Wamel, W., De Groot, N., and Van Belkum, A. (2009). Intestinal carriage of Staphylococcus aureus: how does its frequency compare with that of nasal carriage and what is its clinical impact? Eur. J. Clin. Microbiol. Infect. Dis. *28*, 115–127.

Adams, M.N., Ramachandran, R., Yau, M.-K., Suen, J.Y., Fairlie, D.P., Hollenberg, M.D., and Hooper, J.D. (2011). Structure, function and pathophysiology of protease activated receptors. Pharmacol. Ther. *130*, 248–282.

Bader, M., Alenina, N., Andrade-Navarro, M.A., and Santos, R.A. (2014). Mas and its related G protein-coupled receptors, Mrgprs. Pharmacol. Rev. *66*, 1080–1105.

Bautzova, T., Hockley, J.R.F., Perez-Berezo, T., Pujo, J., Tranter, M.M., Desormeaux, C., Barbaro, M.R., Basso, L., Le Faouder, P., Rolland, C., et al. (2018). 5-oxoETE triggers nociception in constipation-predominant irritable bowel syndrome through MAS-related G protein–coupled receptor D. Sci. Signal. *11*, eaal2171.

Bercik, P., Denou, E., Collins, J., Jackson, W., Lu, J., Jury, J., Deng, Y., Blennerhassett, P., MacRi, J., McCoy, K.D., et al. (2011). The intestinal microbiota affect central levels of brain-derived neurotropic factor and behavior in mice. Gastroenterology *141*, 599–609.e3.

Bharwani, A., West, C., Champagne-Jorgensen, K., McVey Neufeld, K.A., Ruberto, J., Kunze, W.A., Bienenstock, J., and Forsythe, P. (2020). The vagus nerve is necessary for the rapid and widespread neuronal activation in the brain following oral administration of psychoactive bacteria. Neuropharmacology *170*, 108067.

Bhattarai, Y., Williams, B.B., Battaglioli, E.J., Whitaker, W.R., Till, L., Grover, M., Linden, D.R., Akiba, Y., Kandimalla, K.K., Zachos, N.C., et al. (2018). Gut microbiota-produced tryptamine activates an epithelial G-protein-coupled receptor to increase colonic secretion. Cell Host Microbe *23*, 775–785.e5.

Blake, K.J., Baral, P., Voisin, T., Lubkin, A., Pinho-Ribeiro, F.A., Adams, K.L., Roberson, D.P., Ma, Y.C., Otto, M., Woolf, C.J., et al. (2018). Staphylococcus aureus produces pain through pore-forming toxins and neuronal TRPV1 that is silenced by QX-314. Nat. Commun. *9*, 37.

Bravo, J.A., Forsythe, P., Chew, M.V., Escaravage, E., Savignac, H.M., Dinan, T.G., Bienenstock, J., and Cryan, J.F. (2011). Ingestion of Lactobacillus strain regulates emotional behavior and central GABA receptor expression in a mouse via the vagus nerve. Proc. Natl. Acad. Sci. U S A *108*, 16050–16055.

Brierley, S.M., and Linden, D.R. (2014). Neuroplasticity and dysfunction after gastrointestinal inflammation. Nat. Rev. Gastroenterol. Hepatol. *11*, 611–627.

Buhner, S., Li, Q., Vignali, S., Barbara, G., De Giorgio, R., Stanghellini, V., Cremon, C., Zeller, F., Langer, R., Daniel, H., et al. (2009). Activation of human enteric neurons by supernatants of colonic biopsy specimens from patients with irritable bowel syndrome. Gastroenterology *137*, 1425–1434.

Buhner, S., Hahne, H., Hartwig, K., Li, Q., Vignali, S., Ostertag, D., Meng, C., Hörmannsperger, G., Braak, B., Pehl, C., et al. (2018). Protease signaling through protease activated receptor 1 mediate nerve activation by mucosal supernatants from irritable bowel syndrome but not from ulcerative colitis patients. PLoS One *13*, e0193943.

Burgui, S., Gil, C., Solano, C., Lasa, I., and Valle, J. (2018). A systematic evaluation of the two-component systems network reveals that ArlRS is a key regulator of catheter colonization by Staphylococcus aureus. Front. Microbiol. *9*, 342.

Campaniello, M.A., Mavrangelos, C., Eade, S., Harrington, A.M., Blackshaw, L.A., Brierley, S.M., Smid, S.D., and Hughes, P.A. (2017). Acute colitis chronically alters immune infiltration mechanisms and sensory neuro-immune interactions. Brain Behav. Immun. *60*, 319–332.

Cardot-Martin, E., Casalegno, J.S., Badiou, C., Dauwalder, O., Keller, D., Prévost, G., Rieg, S., Kern, W.V., Cuerq, C., Etienne, J., et al. (2015). α-Defensins partially protect human neutrophils against Panton-Valentine leukocidin produced by Staphylococcus aureus. Lett. Appl. Microbiol. *61*, 158–164.

Castro, J., Harrington, A.M., Lieu, T.M., Garcia-Caraballo, S., Maddern, J., Schober, G., O'Donnell, T., Grundy, L., Lumsden, A.L., Miller, P., et al. (2019). Activation of pruritogenic TGR5, MRGPRA3, and MRGPRC11 on colon-innervating afferents induces visceral hypersensitivity. JCI Insight *4*, e131712.

Cenac, N. (2013). Protease-activated receptors as therapeutic targets in visceral pain. Curr. Neuropharmacol. *11*, 598–605.

Cenac, N., Andrews, C.N., Holzhausen, M., Chapman, K., Cottrell, G., Andrade-Gordon, P., Steinhoff, M., Barbara, G., Beck, P., Bunnett,

N.W., et al. (2007). Role for protease activity in visceral pain in irritable bowel syndrome. J. Clin. Invest. *117*, 636–647.

Chang, C., and Lin, H. (2016). Dysbiosis in gastrointestinal disorders. Best Pract. Res. Clin. Gastroenterol. *30*, 3–15.

Chapman, J.R., Balasubramanian, D., Tam, K., Askenazi, M., Copin, R., Shopsin, B., Torres, V.J., and Ueberheide, B.M. (2017). Using quantitative spectrometry to understand the influence of genetics and nutritional perturbations on the virulence potential of Staphylococcus aureus. Mol. Cell. Proteomics *16*, S15–S28.

Chiu, I.M., Heesters, B.A., Ghasemlou, N., Von Hehn, C.A., Zhao, F., Tran, J., Wainger, B., Strominger, A., Muralidharan, S., Horswill, A.R., et al. (2013). Bacteria activate sensory neurons that modulate pain and inflammation. Nature *501*, 52–57.

Cohen, L.J., Esterhazy, D., Kim, S.H., Lemetre, C., Aguilar, R.R., Gordon, E.A., Pickard, A.J., Cross, J.R., Emiliano, A.B., Han, S.M., et al. (2017). Commensal bacteria make GPCR ligands that mimic human signalling molecules. Nature *549*, 48–53.

David, L.A., Maurice, C.F., Carmody, R.N., Gootenberg, D.B., Button, J.E., Wolfe, B.E., Ling, A.V., Devlin, A.S., Varma, Y., Fischbach, M.A., et al. (2014). Diet rapidly and reproducibly alters the human gut microbiome. Nature *505*, 559–563.

Delmas, P., Hao, J., and Rodat-Despoix, L. (2011). Molecular mechanisms of mechanotransduction in mammalian sensory neurons. Nat. Rev. Neurosci. *12*, 139–153.

Denayer, S., Delbrassinne, L., Nia, Y., and Botteldoorn, N. (2017). Food-borne outbreak investigation and molecular typing: high diversity of Staphylococcus aureus strains and importance of toxin detection. Toxins (Basel). *9*, 407.

Dinic, M., Pecikoza, U., Djokic, J., Stepanovic-Petrovic, R., Milenkovic, M., Stevanovic, M., Filipovic, N., Begovic, J., Golic, N., and Lukic, J. (2018). Exopolysaccharide produced by probiotic strain lactobacillus paraplantarum BGCG11 reduces inflammatory hyperalgesia in rats. Front. Pharmacol. *9*, 1.

Feng, B.S., He, S.H., Zheng, P.Y., Wu, L., and Yang, P.C. (2007). Mast cells play a crucial role in Staphylococcus aureus peptidoglycan-induced diarrhea. Am. J. Pathol. *171*, 537–547.

Fey, P.D., Endres, J.L., Yajjala, V.K., Widhelm, T.J., Boissy, R.J., Bose, J.L., and Bayles, K.W. (2013). A genetic resource for rapid and comprehensive phenotype screening of nonessential Staphylococcus aureus genes. MBio *4*, e00537-12.

Fülling, C., Dinan, T.G., and Cryan, J.F. (2019). Gut microbe to brain signaling: what happens in vagus…. Neuron *101*, 998–1002.

Furness, J.B., Rivera, L.R., Cho, H.J., Bravo, D.M., and Callaghan, B. (2013). The gut as a sensory organ. Nat. Rev. Gastroenterol. Hepatol. *10*, 729–740.

Gong, J., Bai, T., Zhang, L., Qian, W., Song, J., and Hou, X. (2017). Inhibition effect of Bifidobacterium longum , Lactobacillus acidophilus , Streptococcus thermophilus and Enterococcus faecalis and their related products on human colonic smooth muscle in vitro. PLoS One *12*, 1–15.

Gourbeyre, P., Berri, M., Lippi, Y., Meurens, F., Vincent-Naulleau, S., Laffitte, J., Rogel-Gaillard, C., Pinton, P., and Oswald, I.P. (2015). Pattern recognition receptors in the gut: analysis of their expression along the intestinal tract and the crypt/villus axis. Physiol. Rep. *3*, e12225.

Guarino, M.P., Altomare, A., Stasi, E., Marignani, M., Severi, C., Alloni, R., Dicuonzo, G., Morelli, L., Coppola, R., and Cicala, M. (2008). Effect of acute mucosal exposure to Lactobacillus rhamnosus GG on human colonic smooth muscle cells. J. Clin. Gastroenterol. *42* (*Suppl 3 Pt 2*), S185–S190.

Gupta, K., and Harvima, I.T. (2018). Mast cell-neural interactions contribute to pain and itch. Immunol. Rev. *282*, 168–187.

Hockley, J.R.F., Taylor, T.S., Callejo, G., Wilbrey, A.L., Gutteridge, A., Bach, K., Winchester, W.J., Bulmer, D.C., McMurray, G., and Smith, E.S.J. (2018). Single-cell RNAseq reveals seven classes of colonic sensory neuron. Gut *68*, 633–644.

von Hoven, G., Rivas, A.J., Neukirch, C., Klein, S., Hamm, C., Qin, Q., Meyenburg, M., Fuser, S., Saftig, P., Hellmann, N., et al. (2016). Dissecting the role of ADAM10 as a mediator of Staphylococcus aureus -toxin action. Biochem. J. *473*, 1929–1940.

Hughes, P.A., Harrington, A.M., Castro, J., Liebregts, T., Adam, B., Grasby, D.J., Isaacs, N.J., Maldeniya, L., Martin, C.M., Persson, J., et al. (2013). Sensory neuro-immune interactions differ between Irritable Bowel Syndrome subtypes. Gut *62*, 1456–1465.

Ibeakanma, C., and Vanner, S. (2010). TNFα is a key mediator of the pronociceptive effects of mucosal supernatant from human ulcerative colitis on colonic DRG neurons. Gut *59*, 612–621.

Ibeakanma, C., Ochoacortes, F., Mirandamorales, M., McDonald, T., Spreadbury, I., Cenac, N., Cattaruzza, F., Hurlbut, D., Vanner, S., Bunnett, N., et al. (2011). BrainGut interactions increase peripheral nociceptive signaling in mice with postinfectious irritable bowel syndrome. Gastroenterology *141*, 2098–2108.e5.

Inoshima, I., Inoshima, N., Wilke, G.A., Powers, M.E., Frank, K.M., Wang, Y., and Wardenburg, J.B. (2011). A Staphylococcus aureus pore-forming toxin subverts the activity of ADAM10 to cause lethal infection in mice. Nat. Med. *17*, 1310–1314.

Kelly, J.R., Minuto, C., Cryan, J.F., Clarke, G., and Dinan, T.G. (2017). Cross talk: the microbiota and neurodevelopmental disorders. Front. Neurosci. *11*, 1–31.

Kolar, S.L., Antonio Ibarra, J., Rivera, F.E., Mootz, J.M., Davenport, J.E., Stevens, S.M., Horswill, A.R., and Shaw, L.N. (2013). Extracellular proteases are key mediators of Staphylococcus aureus virulence via the global modulation of virulence-determinant stability. Microbiologyopen *2*, 18–34.

Korecka, A., Dona, A., Lahiri, S., Tett, A.J., Al-Asmakh, M., Braniste, V., D'Arienzo, R., Abbaspour, A., Reichardt, N., Fujii-Kuriyama, Y., et al. (2016). Bidirectional communication between the Aryl hydrocarbon Receptor (AhR) and the microbiome tunes host metabolism. NPJ Biofilms Microbiomes *2*, 16014.

Laabei, M., Jamieson, W.D., Yang, Y., Van Den Elsen, J., and Jenkins, A.T.A. (2014). Investigating the lytic activity and structural properties of Staphylococcus aureus phenol soluble modulin (PSM) peptide toxins. Biochim. Biophys. Acta *1838*, 3153–3161.

Labandeira-Rey, M., Couzon, F., Boisset, S., Brown, E.L., Bes, M., Benito, Y., Barbu, E.M., Vazquez, V., Höök, M., Etienne, J., et al. (2007). Staphylococcus aureus Panton-Valentine leukocidin causes necrotizing pneumonia. Science *315*, 1130–1133.

Lai, N.Y., Mills, K., and Chiu, I.M. (2017). Sensory neuron regulation of gastrointestinal inflammation and bacterial host defence. J. Intern. Med. *282*, 5–23.

LaSarre, B., and Federle, M.J. (2013). Exploiting quorum sensing to confuse bacterial pathogens. Microbiol. Mol. Biol. Rev. *77*, 73–111.

Los, F.C.O., Randis, T.M., Aroian, R.V., and Ratner, A.J. (2013). Role of pore-forming toxins in bacterial infectious diseases. Microbiol. Mol. Biol. Rev. *77*, 173–207.

Mao, Y.K., Kasper, D.L., Wang, B., Forsythe, P., Bienenstock, J., and Kunze, W.A. (2013). Bacteroides fragilis polysaccharide A is necessary and sufficient for acute activation of intestinal sensory neurons. Nat. Commun. *4*, 1465.

Massi, M., Ioan, P., Budriesi, R., Chiarini, A., Vitali, B., Lammers, K.M., Gionchetti, P., Campieri, M., Lembo, A., and Brigidi, P. (2006). Effects of probiotic bacteria on gastrointestinal motility in Guinea-pig isolated tissue. World J. Gastroenterol. *12*, 5987–5994.

Menestrina, G. (1986). Ionic channels formed by Staphylococcus aureus alpha-toxin: voltage-dependent inhibition by divalent and trivalent cations. J. Membr. Biol. *90*, 177–190.

Mukherjee, S., and Bassler, B.L. (2019). Bacterial quorum sensing in complex and dynamically changing environments. Nat. Rev. Microbiol. *17*, 371–382.

Nakamura, Y., Oscherwitz, J., Cease, K.B., Chan, S.M., Muñoz-Planillo, R., Hasegawa, M., Villaruz, A.E., Cheung, G.Y.C., McGavin, M.J., Travers, J.B., et al. (2013). Staphylococcus δ-toxin induces allergic skin disease by activating mast cells. Nature *503*, 397–401.

Nakao, A., Ito, T., Han, X., Lu, Y.J., Hisata, K., Tsujiwaki, A., Matsunaga, N., Komatsu, M., Hiramatsu, K., and Shimizu, T. (2014). Intestinal carriage of methicillin-resistant Staphylococcus aureus in nasal MRSA carriers hospitalized in the neonatal intensive care unit. Antimicrob. Resist. Infect. Control *3*, 14.

Obata, Y., Castaño, Á., Boeing, S., Bon-Frauches, A.C., Fung, C., Fallesen, T., de Agüero, M.G., Yilmaz, B., Lopes, R., Huseynova, A., et al. (2020). Neuronal programming by microbiota regulates intestinal physiology. Nature *578*, 284–289.

Ochoa-Cortes, F., Ramos-Lomas, T., Miranda-Morales, M., Spreadbury, I., Ibeakanma, C., Barajas-Lopez, C., and Vanner, S. (2010). Bacterial cell products signal to mouse colonic nociceptive dorsal root ganglia neurons. Am. J. Physiol. Gastrointest. Liver Physiol. *299*, G723–G732.

Peeters, P.J., Aerssens, J., de Hoogt, R., Stanisz, A., Göhlmann, H.W., Hillsley, K., Meulemans, A., Grundy, D., Stead, R.H., and Coulie, B. (2006). Molecular profiling of murine sensory neurons in the nodose and dorsal root ganglia labeled from the peritoneal cavity. Physiol. Genomics *24*, 252–263.

Piewngam, P., Zheng, Y., Nguyen, T.H., Dickey, S.W., Joo, H.S., Villaruz, A.E., Glose, K.A., Fisher, E.L., Hunt, R.L., Li, B., et al. (2018). Pathogen elimination by probiotic Bacillus via signalling interference. Nature *562*, 532–537.

Pokusaeva, K., Johnson, C., Luk, B., Uribe, G., Fu, Y., Oezguen, N., Matsunami, R.K., Lugo, M., Major, A., Mori-Akiyama, Y., et al. (2017). GABA-producing Bifidobacterium dentium modulates visceral sensitivity in the intestine. Neurogastroenterol. Motil. *29*, 1–14.

Rautenberg, M., Joo, H.-S., Otto, M., and Peschel, A. (2011). Neutrophil responses to staphylococcal pathogens and commensals via the formyl peptide receptor 2 relates to phenol-soluble modulin release and virulence. FASEB J. *25*, 1254–1263.

Rinttilä, T., Lyra, A., Krogius-Kurikka, L., and Palva, A. (2011). Real-time PCR analysis of enteric pathogens from fecal samples of irritable bowel syndrome subjects. Gut Pathog. *3*, 6.

Rong, W., Hillsley, K., Davis, J.B., Hicks, G., Winchester, W.J., and Grundy, D. (2004). Jejunal afferent nerve sensitivity in wild-type and TRPV1 knockout mice. J. Physiol. *560*, 867–881.

Sanders, K.M., Koh, S.D., Ro, S., and Ward, S.M. (2012). Regulation of gastrointestinal motility- - insights from smooth muscle biology. Nat. Rev. Gastroenterol. Hepatol. *9*, 633–645.

Schreiner, J., Kretschmer, D., Klenk, J., Otto, M., Buhring, H.-J., Stevanovic, S., Wang, J.M., Beer-Hammer, S., Peschel, A., and Autenrieth, S.E. (2013). Staphylococcus aureus phenol-soluble modulin peptides modulate dendritic cell functions and increase in vitro priming of regulatory T cells. J. Immunol. *190*, 3417–3426.

Sessenwein, J.L., Baker, C.C., Pradhananga, S., Maitland, M.E., Petrof, E.O., Allen-Vercoe, E., Noordhof, C., Reed, D.E., Vanner, S.J., and Lomax, A.E. (2017). Protease-mediated suppression of DRG neuron excitability by commensal bacteria. J. Neurosci. *37*, 11758–11768.

Song, J., Zhang, L., Bai, T., Qian, W., Li, R., and Hou, X. (2015). Mast cell-dependent mesenteric afferent activation by mucosal supernatant from different bowel segments of Guinea pigs with post-infectious irritable bowel syndrome. J. Neurogastroenterol. Motil. *21*, 236–246.

Song, D., Meng, J., Cheng, J., Fan, Z., Chen, P., Ruan, H., Tu, Z., Kang, N., Li, N., Xu, Y., et al. (2018). Pseudomonas aeruginosa quorum-sensing metabolite induces host immune cell death through cell surface lipid domain dissolution. Nat. Microbiol. *4*, 97–111.

Spaan, A.N., van Strijp, J.A.G., and Torres, V.J. (2017). Leukocidins: staphylococcal bi-component pore-forming toxins find their receptors. Nat. Rev. Microbiol. *15*, 435–447.

Strandwitz, P., Kim, K.H., Terekhova, D., Liu, J.K., Sharma, A., Levering, J., McDonald, D., Dietrich, D., Ramadhar, T.R., Lekbua, A., et al. (2019). GABA-modulating bacteria of the human gut microbiota. Nat. Microbiol. *4*, 396–403.

Tam, K., and Torres, V.J. (2019). Staphylococcus aureus Secreted Toxins and Extracellular Enzymes. Microbiol. Spectr. *7*, https://doi.org/10.1128/microbiolspec.GPP3-0039-2018.

Valdez-Morales, E.E., Overington, J., Guerrero-Alba, R., Ochoa-Cortes, F., Ibeakanma, C.O., Spreadbury, I., Bunnett, N.W., Beyak, M., and Vanner, S.J. (2013). Sensitization of peripheral sensory nerves by mediators from colonic biopsies of diarrhea-predominant irritable bowel syndrome patients: a role for PAR2. Am. J. Gastroenterol. *108*, 1634–1643.

Vandenesch, F., Lina, G., and Henry, T. (2012). Staphylococcus aureus hemolysins, bi-component leukocidins, and cytolytic peptides: a redundant arsenal of membrane-damaging virulence factors? Front. Cell. Infect. Microbiol. *2*, 12.

Virreira Winter, S., Zychlinsky, A., and Bardoel, B.W. (2016). Genome-wide CRISPR screen reveals novel host factors required for Staphylococcus aureus α-hemolysin-mediated toxicity. Sci. Rep. *6*, 24242.

Wang, B., Mao, Y.K., Diorio, C., Pasyk, M., Wu, R.Y., Bienenstock, J., and Kunze, W.A. (2010). Luminal administration ex vivo of a live Lactobacillus species moderates mouse jejunal motility within minutes. FASEB J. *24*, 4078–4088.

Wang, R., Braughton, K.R., Kretschmer, D., Bach, T.H.L., Queck, S.Y., Li, M., Kennedy, A.D., Dorward, D.W., Klebanoff, S.J., Peschel, A., et al. (2007). Identification of novel cytolytic peptides as key virulence determinants for community-associated MRSA. Nat. Med. *13*, 1510–1514.

Wilke, G.A., and Wardenburg, J.B. (2010). Role of a disintegrin and metalloprotease 10 in Staphylococcus aureus -hemolysin-mediated cellular injury. Proc. Natl. Acad. Sci. U S A *107*, 13473–13478.

Woolf, C.J. (2018). Pain amplification-A perspective on the how, why, when, and where of central sensitization. J. Appl. Biobehav. Res. *23*, e12124.

iScience, Volume *23*

Supplemental Information

Identification of a Quorum Sensing-Dependent Communication Pathway Mediating Bacteria-Gut-Brain Cross Talk

Friederike Uhlig, Luke Grundy, Sonia Garcia-Caraballo, Stuart M. Brierley, Simon J. Foster, and David Grundy

Supplemental Data

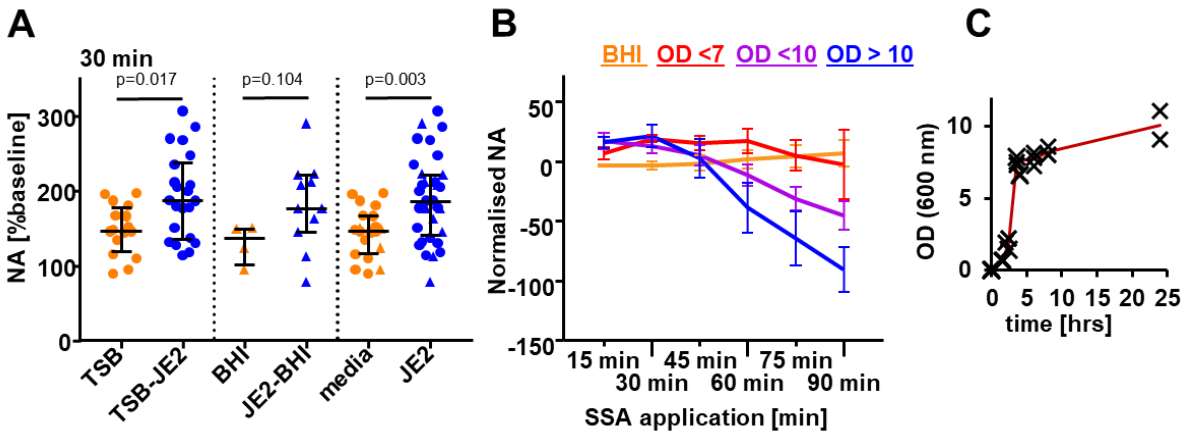

Figure S1: Effect of growth stage on nerve response profile to SSA, Related to Figure 1, Figure 2, Figure 3.

A) Comparison of the excitatory effect of SSA-JE2 produced in two different bacterial growth media. SSA prepared in tryptic soy broth (TSB) significantly increased nerve activity (NA) relative to vehicle. The difference between brain heart infusion buffer (BHI) and SSA-JE2 prepared in this growth medium was not significantly different. The pairwise comparisons between TSB and BHI as well as JE2-TSB and JE2-BHI were not significantly different.
Data are median ± interquartile range. N(TSB) = 17, N(TSB-JE2) = 22, N(BHI) = 4, N(BHI-JE2) = 11, Two-sided Mann-Whitney Tests
B) Data presented in Fig 2 was analysed by optical density (as an estimate for bacterial growth) of SSA rather than time of incubation. SSA with high optical density decreased nerve activity during long-term application. This inhibition was reduced when SSA with lower optical density were applied.
Data are median ± interquartile range. N(BHI) = 4, N(OD<7) = 6, N(OD <10) = 32, N(OD>10) = 21
C) Correlation of optical density and time of incubation. After a lag phase, bacteria enter exponential growth stage by about 3 hours and during that time optical density increases rapidly from OD = 2 to OD = 7. Longer incubation reduces the growth rate (increase of OD) and optical density plateaus. This is referred to as stationary phase.

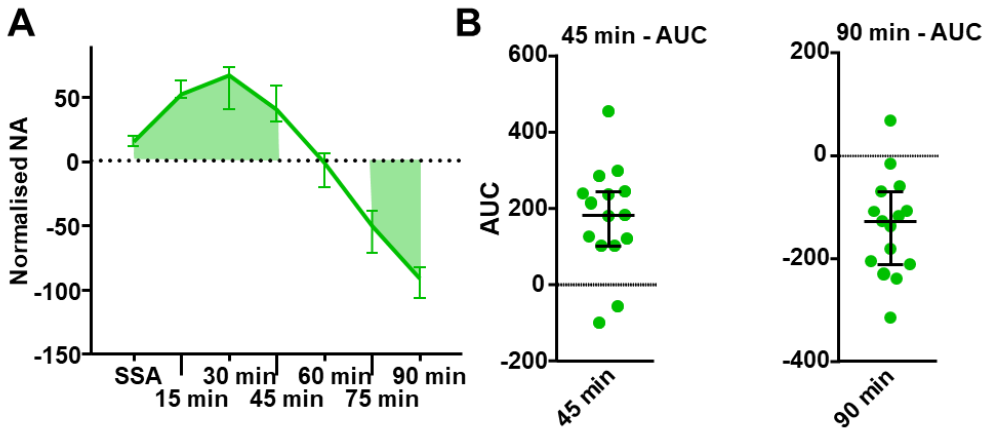

Figure S2: SSA-(20 % v/v)-induced changes of nerve activity, Related to Figure 1, Figure 2, Figure 3

A) Example trace for N = 15 preparations and how the integrated excitatory activity (**B,** left) and inhibitory activity (**B,** right) were calculated as area under the curve (AUC). NA: nerve activity. Data are median ± interquartile range.

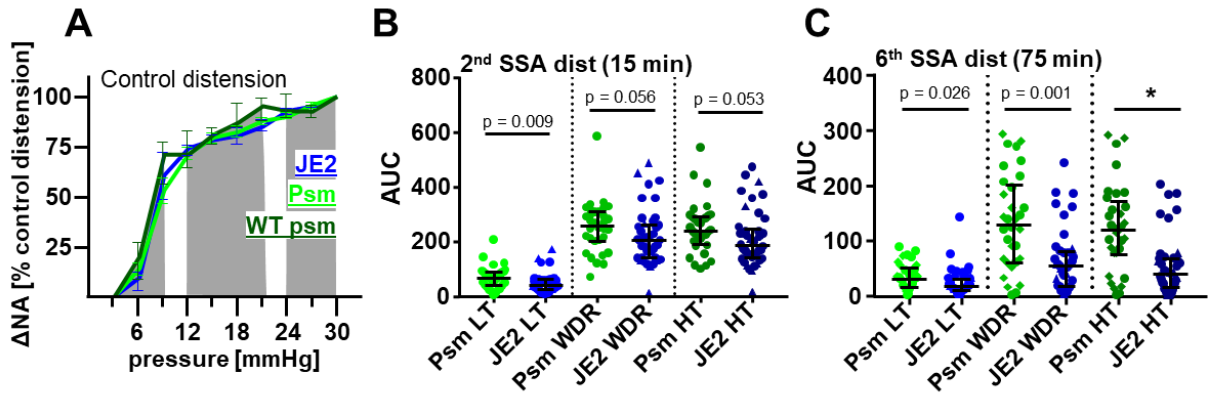

Figure S3: Psms contribute to the inhibition of mechanosensitivity induced by SSA-JE2, Related to Figure 3.

A) The distension response profile of small intestinal nerves before application of SSA is characterized by the sequential activation of low threshold (LT), wide dynamic range (WDR) and high threshold (HT) afferent fibres. The effect of SSA on these aspects of mechanosensitivity were investigated by integrating the pressure-induced increase of afferent discharge as depicted.

B) Comparison of distension-induced firing 15 min after SSA-psm$^-$ or SSA-JE2 application. Only the mechanosensitivity of the LT component was differently affected by SSA-psm$^-$ and SSA-JE2. The higher activity indicates a reduction of the SSA-JE2 induced inhibition of mechanosensitivity. A similar trend was observed for WDR and HT components but the SSA-induced alteration of mechanosensitivity was not significantly different between SSA lacking psm and wildtype suggesting that psms in SSA-JE2 have a bigger impact on low threshold fibres during short term application.

C) Distension-induced firing of LT, WDR and HT components was significantly higher when SSA lacking psms were applied for 75 min which means that the extent of SSA-JE2-induced inhibition of mechanosensitivity is dependent on the abundance of psms. In a small number of experiments with SSA-psm$^-$, the distension response of WDR and HT component was reduced to a similar degree as in experiments with SSA-JE2.

Data from experiments where SSA-psm$^-$ inhibited spontaneous firing are indicated as squares. The distension response of JE2 represents SSA-JE2 (circles) and SSA from the wildtype used for the generation of the psm-deficient JE2 (triangles). There was no significant difference between these two variants of JE2.

AUC: area under the curve. Data are median ± interquartile range. Non-parametrical statistical analysis (Two-sided Mann-Whitney test) was performed on data from N(Psm$^-$) = 32, N(JE2) = 37

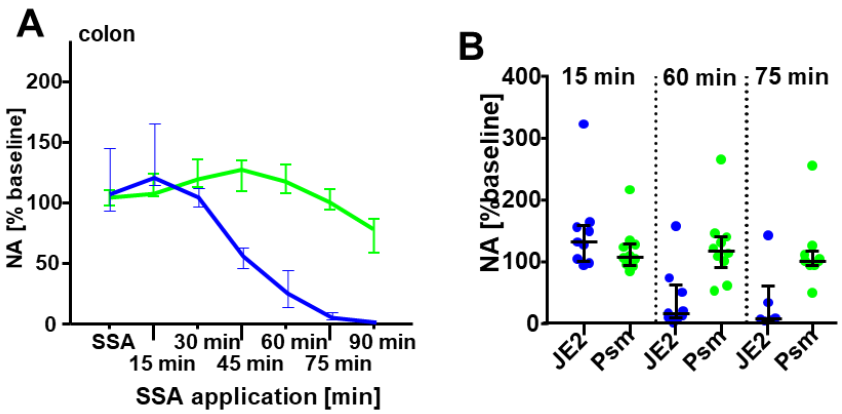

Figure S4: Response of nerves innervating the proximal colon to SSA, related to Figure 2, Figure 3

A) Response profile of colonic afferent nerves to SSA-JE2 and SSA-psm$^-$. Data for SSA-JE2 was obtained from animals in Sheffield. Experiments with SSA-psm$^-$ were performed at SAHMRI. As in the small intestine, the response profiles induced by SSA-JE2 and SSA-psm$^-$ were different. Nerve activity was normalised to baseline before SSA application.

B) Comparison of the early (left part of the panel) and late (right part of the panel) effect of SSAs on colonic afferents. There was no statistical difference with regard to the excitatory effect of SSA-JE2 and SSA-psm$^-$. The SSA-induced changes of nerve activity during long term application were significantly different although the response to SSA-psm$^-$ was also variable.

Data are median ± interquartile range. Non-parametric statistical analysis (Two-sided Mann-Whitney Test) was performed per time point on data from N(JE2) = 9, N(Psm) = 11 mice, one recording per mouse

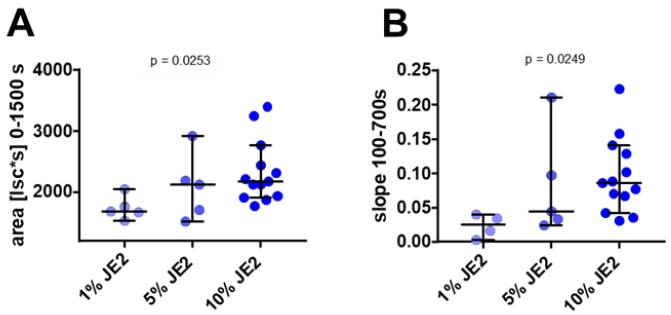

Figure S5: Serosal application of SSA increases short circuit currents, Related to Figure 5
Different concentrations (v/v) of SSA-JE2 were applied to mucosa-submucosa preparations from mouse small intestine in Ussing Chambers. The area under the curve **(A)** and the slope **(B)** were significantly increased.
Data are median ± interquartile range N(1 %) = 5 preparations, N(5 %) = 5 preparations, N(10 %) = 13 preparations from seven animals, p value represents Kruskall Wallis statistic

Transparent Methods

Mice

In this study, experiments were performed at the University of Sheffield (UK) and the South Australian Health and Medical Research Institute (SAHMRI, Adelaide, Australia). All animal experiments were performed according to the Animal Scientific Procedure Act 1986 (UK) and approved by the Animal Ethics Committee of The University of Adelaide (Australia) and Sheffield (UK). Throughout the study, adult male C57Bl/6J mice (10-20 weeks) were used and kept under specific pathogen-free conditions. They were fed a standard chow with free access to water and housed in group cages with up to 5 animals. Male mice were used for this study to avoid any confounding influences resulting from variations in gut function and sensory signalling during the oestrus cycle (Hogan et al., 2012).

Retrograde tracing from the viscera

AlexaFluor488-conjugated cholera toxin subunit B (CTB-488, 250 µg) was injected into the lower left abdominal quadrant of anaesthetised C57Bl/6 (2-4 % isoflurane) animals to enable identification of neurons that innervate the intestine for PI live imaging and qRT-PCR (Peeters et al., 2006). Mice were subcutaneously injected with analgesic (Buprenorphine; 2.7 µg/30 g) and antibiotic (Ampicillin; 50 mg/kg) as they regained consciousness and housed individually for 3-5 days. IP injection of tracer has been validated previously by our group and was chosen because it labels the majority of intestine-innervating neurons without any surgery-induced phenotypic changes. Then, animals were subsequently euthanised using CO_2 and exsanguination (Australian animal regulation) and retrogradely-labelled neurons were readily identifiable in the harvested ganglia.

Afferent nerve recordings

C57Bl/6J mice were humanly killed by isoflurane inhalation followed by cervical dislocation (UK) or increasing CO_2 exposure and exsanguination (Australia). The intestine was removed from the animal and placed into Krebs solution (mM: NaCl 120, KCl 5.9, $MgSO_4$ 1.2, NaH_2PO_4 1.2, $NaHCO_3$ 15.4, glucose 11.5, and $CaCl_2$ 1.2) that was gassed with carbogen (95 % O_2/5 % CO_2). Afferent nerve activity was recorded from nerves innervating the distal small intestine or proximal colon as previously described (Rong et al., 2004). The segment (3-4 cm) with the attached mesenteric bundles was isolated, the ingesta was gently removed, and placed into an organ bath chamber that was continuously perfused with carbogenated Krebs solution. Both ends of the segment were cannulated to allow continuous intraluminal perfusion. One mesenteric nerve bundle was dissected and placed into the recording “suction” electrode. Nerve activity was recorded using the Neurolog system (Neurolog headstage NL 100, amplifier NL104 and filter NL125), a Micro1401 digitiser and Spike2 software (CED Cambridge). Distensions were induced by closing a tap that was connected to the anal end of the intraluminal perfusion system. Intraluminal pressure was measured simultaneously and monitored during distension. When

intraluminal pressure reached 30 mmHg, the tap was opened to allow free-drainage of the accumulated fluid.

After a 45-60 min stabilisation period and at last two reproducible distensions, bacteria-free growth media (BF-GM) and supernatants of *S. aureus* cultures (SSA) were bath-applied for 15 and 90 min respectively during which time tissue was distended every 15 min. The SSA-induced changes of afferent nerve activity (NA) were quantified relative to control; i.e. the spontaneous discharge under baseline conditions (Krebs perfusion). The effect of vehicle (BF-GM) was determined accordingly and subtracted from the effect of SSA (normalised NA, Fig S2) to account for the BF-GM-induced increase (up to about 150 % baseline nerve activity, Fig. 1, S1) in each individual segment. The afferent response to distension was quantified in pressure intervals of 3 mmHg using a script kindly provided by CED Cambridge. The pressure-induced increase of afferent firing during SSA or vehicle application was calculated as a percentage of the maximal distension response induced by distension to 30 mmHg under control conditions (ΔNA [% control distension]).

Preparation of supernatants

Supernatants from mutants of *S. aureus* strain JE2 were prepared by inoculating sterile bacterial growth media (tryptic soy broth, TSB) with single colonies from the respective bacteria grown on TSB agar plates. For some bacteria, antibiotics were added to the plates (ΔPsm: spectinomycin, Δproteases: erythromycin) to select for the desired genotype (Kolar et al., 2013, Wang et al., 2007). Starting cultures were grown overnight (37 °C on a rotary shaker), after which there were only minor differences in optical density reflecting similar bacterial density for the various mutants. In order to standardise between experiments the overnight cultures were diluted to an OD_{600} of 0.150 in a 2 L flask. These flasks were incubated for 24 hours (unless stated otherwise) under the same conditions. Centrifugation was used to remove the bacteria and supernatants were stored in 50 mL Falcon tubes at -20 °C until usage. In addition, some nerve recording experiments were performed using brain-heart infusion (BHI) growth medium instead of TSB. SSA prepared in BHI exhibited a similar response pattern as SSA prepared in TSB (Fig S1) with higher variability especially in the initial excitatory response.

When SSA were used in electrophysiology or motility experiments, they were defrosted in a warm water bath and diluted in Krebs buffer (1:20, 5 % v/v for motility and 1:5, 20 % v/v for electrophysiology). They were bath-applied as indicated by exchanging the Krebs buffer in the reservoir for the diluted SSA.
For Ussing Chamber and propidium iodide (PI) experiments, SSA were passed through a sterile filter before usage. Filtered samples were aliquoted and frozen. Before usage, SSA were defrosted at room temperature and diluted in Krebs (Ussing chamber) or HEPES buffer (composition in mM: HEPES [2-hydroxyethyl-1-piperazine-ethanesulfonic acid] 10, NaCl 142, KCl 2, glucose 10, $CaCl_2$ 2, pH adjusted to 7.4 with NaOH) (PI live imaging) by volume.

Isolation of dorsal root and nodose ganglia

Naïve animals or animals that had been injected with the retrograde tracing dye were humanely killed and the nodose ganglia and dorsal root ganglia from the excised spinal cord were dissected and placed into ice-cold Hanks balanced salt solution (HBSS) for primary cultures or frozen (-80 °C) for expression analysis. Thoracolumbar (T9-L1) and lumbosacral (L6-S1) regions of the spinal cord were marked with a small incision prior to removal of the spinal cord.

Primary cultures of DRG and NG neurons

Primary culture of ganglia was performed as previously described(Grundy et al., 2018b, Grundy et al., 2018a, Grundy et al., 2018c). Ganglia were enzymatically digested at 37 °C (30 min 4 mg/mL collagenase + 4 mg/mL dispase, 10 min 4 mg/mL collagenase type II only, GIBCO). Afterwards, ganglia were washed twice with HBSS and triturated using fire-polished glass pipettes with descending diameter. Suspensions were centrifuged and the cell pellet resolved in about 300 µL culturing media (DMEM [Dulbecco's Modified Eagle Medium] supplemented with 10 % FBS, 1 % P/S, glutamine, 0.1 µg/mL NGF-7S). 20 µL were plated on poly-D-lysine- (800 µg/mL) and laminin (20 µg/mL) -coated 13 mm glass coverslips. Cultures were flooded two hours after plating with culturing media.

For expression analysis, traced NG, TL or LS DRG neurons were manually selected under a fluorescence microscope using a blunted glass pipette mounted onto a micromanipulator within 24 hours after isolation (Castro et al., 2019, Grundy et al., 2020). Pipette tips were crushed into RNA lysis buffer (10 µL) and pooled (200 µL) to investigate a potential selective expression of *Fprs*, *Adam10* and *Sgms1* in these neurons.

Live Cell Imaging

We performed live cell imaging with propidium iodide (PI) on primary cultures of DRG and NG neurons to investigate the effect of SSA on cell membrane permeability. PI staining is traditionally used to assess cell viability but it is increasingly recognised that the an increase of cell membrane permeability for PI does not necessarily indicate cell death (Torres et al., 2017, Whalen et al., 2008). For live imaging, neurons were pre-incubated with PI (PI 1 mg/mL diluted 1:1.000 in HEPES buffer) for 20 min. Then, the coverslip was mounted on to the recording chamber and cells washed with HEPES using a hand-made perfusion system. Then, cells were incubated with HEPES buffer (+PI) for 10 min and subsequently, SSA diluted in HEPES (+PI) were perfused for 3 min. The perfusion was stopped and the cells incubated with SSA for another 27 min during which they were continuously imaged. Images were taken every 5 s using the 20x objective of a Nikon TE300 Eclipse microscope equipped with a Sutter DG-4/OF wavelength switcher and connected to Photonic Science ISIS-3 intensified CCD camera with Universal Interface Card Data for data acquisition with MetaFluor software. Regions of interest were selected based on cell shape and PI staining. Only data from cells that displayed neuronal morphology and no intracellular PI was recorded and further analysed with MicrosoftExcel®.

After subtraction of baseline, two parameters were calculated to compare the effects between different SSA. Firstly, Δfluorescence was used as an indicator for the overall effect of SSA and constitutes the average of SSA-induced fluorescence from all selected cells per coverslip. Secondly, response latencies were determined for responding cells which were identified based on the increase of PI fluorescence. Because the lowest concentration of SSA (0.1 %) or 20 % of vehicle did not increase Δfluorescence further than 15, this value was used as threshold to calculate the response latency as the time difference between the start of application and crossing the threshold value.

Expression analysis

Segments from the distal intestine in PBS were defrosted and RNA isolated using PureLink® RNA Mini kit. For whole DRG, NG and intestine-innervating neurons NucleoSpin® RNA XS kit (Machenery Nagel™) was used because of the small amount of sample RNA. Intestine-innervating neurons were isolated from primary cultures of TL and LS as well as NG neurons obtained from animals that were subjected to retrograde tracing procedures using a glass pipettes on a micromanipulator.
After RNA isolation, expression of target genes (*Fpr1*-3: NM_013521.2, NM_008039.2 and NM_008042.2, *Adam10*: NM_007399.4, *Sgms1*: NM_001168525.1) and reference genes (*b-actin*, *Gapdh*) was assessed using quantitative reverse transcription PCR with TaqMan® assays (Mm00545742_m1, Mm00522643_m1, Mm00442803_s1, Mm00484464_s1, Mm01962454_s1, Mm99999915_g1, Mm00607939_s1) and EXPRESS One-Step SuperScript® qRT-PCR Kits. Expression of target genes was quantified against the geometric mean of reference genes.

Ussing Chambers

To investigate the effect of SSA on intestinal secretion, we recorded short circuit currents (SCC) in EasyMount Ussing chambers (Physiologic Instruments, San Diego, USA). Mouse small intestinal mucosa-submucosa explants were prepared by removing the muscle layer under a dissection microscope. The explants were placed into the inserts (area 0.1 mm^2) for the recording chambers, both chambers filled with carbogenated Krebs solution and tissues were allowed to stabilise for 45 min. All recordings were performed at 35 °C, using $Ag/AgCl_2$ electrodes in KCl and in remote ("REM" mode) mode. SSA were applied to the serosal side and the same amount of Krebs was pipetted into the luminal chamber to account for volume differences.

Data acquisition was performed using ACQUIRE&ANALYZE (Physiologic Instruments) which determines transepithelial potential (voltage, V), electrogenic transport (current, I) and tissue resistance (R) simultaneously. SSA-induced changes of circuit current (SCC) were quantified relative to baseline after the stabilisation period. Area under the curve was calculated by addition of individual values until 1500 s of application. The slope of the SSA-induced increase was determined between 100 and 700 s of application as: ΔSCC/600 s.

Motility

To record intestinal motility, the proximal colon (3-4 cm) distal from the caecum was dissected from the whole length intestine after its removal from male C57Bl/6J mice. It was flushed with fresh Krebs solution and tied on to the intraluminal perfusion system of an organ bath chamber similar to the one that was used for electrophysiological nerve recordings. The chamber was constantly perfused with carbogenated Krebs and maintained at 33-34 °C. Krebs was also perfused through the lumen at a rate of 300 µL/min during the first 20-30 min to flush the colon of any remaining ingesta. Then, the intraluminal perfusion rate was reduced (100 µL/min) and the outflow tab at the anal end of the perfusion system was closed. Pressure was monitored using a pressure transducer and amplification system that was connected to the anal end using a three-way tab. Once the intraluminal pressure reached 3-5 mmHg, the perfusion was stopped and this small distension induced the generation of migrating motor complexes (MMC) as previously reported (Keating et al., 2010, Keating et al., 2014).

SSA were bath-applied for 60 min after the MMC activity had stabilized. In the subsequent 30 min wash period, Krebs buffer was perfused through the bath. The number and maximal amplitude of contractions within a 15 min interval at the end of the application or wash-out period was determined.

Statistical analysis

Raw data was analysed using Spike2 (electrophysiology, motility), ACQUIRE&ANAYZE (Ussing Chambers) and MetaFluor (PI Imaging) and processed in MicrosoftExcel®. For nerve recording experiments, the overall excitatory activity was calculated by addition of time points during which normalised nerve activity increased (30-45 min) whereas time points with decreased normalised nerve activity (60-90 min) were added for the overall inhibitory activity (area under the curve, AUC, Fig. S2). N numbers represent the number of mice that were used for experimentations. Occasionally, several (up to three) segments/preparations from one mouse were used for nerve recording experiments. In those cases, they were exposed to different SSA and treated as independent samples.

SPSS statistics (version 23, IBM) was used for interpretation and data was extracted and transferred into GraphPad Prism™ 7 for statistical analysis and presentation. Non-parametric statistical analyses were performed and data is depicted as median and interquartile ranges. Data was considered statistically significant if $p < 0.05$. Exact p values are stated where appropriate.

Supplementary References

CASTRO, J., HARRINGTON, A. M., LIEU, T., GARCIA-CARABALLO, S., MADDERN, J., SCHOBER, G., O'DONNELL, T., GRUNDY, L., LUMSDEN, A. L., MILLER, P., GHETTI, A., STEINHOFF, M. S., POOLE, D. P., DONG, X., CHANG, L., BUNNETT, N. W. & BRIERLEY, S. M. 2019. Activation of pruritogenic TGR5, MrgprA3, and MrgprC11 on colon-innervating afferents induces visceral hypersensitivity. *JCI Insight,* 4.

GRUNDY, L., CALDWELL, A., GARCIA CARABALLO, S., ERICKSON, A., SCHOBER, G., CASTRO, J., HARRINGTON, A. M. & BRIERLEY, S. M. 2020. Histamine induces peripheral and central hypersensitivity to bladder distension via the histamine H1 receptor and TRPV1. *Am J Physiol Renal Physiol,* 318**,** F298-F314.

GRUNDY, L., ERICKSON, A., CALDWELL, A., GARCIA-CARABALLO, S., RYCHKOV, G., HARRINGTON, A. & BRIERLEY, S. M. 2018a. Tetrodotoxin-sensitive voltage-gated sodium channels regulate bladder afferent responses to distension. *Pain*.

GRUNDY, L., ERICKSON, A., CALDWELL, A., GARCIA-CARABALLO, S., RYCHKOV, G., HARRINGTON, A. & BRIERLEY, S. M. 2018b. Tetrodotoxin-sensitive voltage-gated sodium channels regulate bladder afferent responses to distension. *Pain,* 159**,** 2573-2584.

GRUNDY, L., HARRINGTON, A. M., CASTRO, J., GARCIA-CARABALLO, S., DEITEREN, A., MADDERN, J., RYCHKOV, G. Y., GE, P., PETERS, S., FEIL, R., MILLER, P., GHETTI, A., HANNIG, G., KURTZ, C. B., SILOS-SANTIAGO, I. & BRIERLEY, S. M. 2018c. Chronic linaclotide treatment reduces colitis-induced neuroplasticity and reverses persistent bladder dysfunction. *JCI Insight,* 3.

HOGAN, A. M., COLLINS, D., BAIRD, A. W. & WINTER, D. C. 2012. Estrogen and its role in gastrointestinal health and disease.

KEATING, C., EWART, L., GRUNDY, L., VALENTIN, J. P. & GRUNDY, D. 2014. Translational potential of a mouse in vitro bioassay in predicting gastrointestinal adverse drug reactions in Phase I clinical trials. *Neurogastroenterology & Motility,* 26**,** 980-989.

KEATING, C., MARTINEZ, V., EWART, L., GIBBONS, S., GRUNDY, L., VALENTIN, J.-P. & GRUNDY, D. 2010. The validation of an invitro colonic motility assay as a biomarker for gastrointestinal adverse drug reactions. *Toxicology and Applied Pharmacology,* 245**,** 299-309.

KOLAR, S. L., IBARRA, J. A., RIVERA, F. E., MOOTZ, J. M., DAVENPORT, J. E., STEVENS, S. M., HORSWILL, A. R. & SHAW, L. N. 2013. Extracellular proteases are key mediators of Staphylococcus aureus virulence via the global modulation of virulence-determinant stability. *Microbiologyopen,* 2**,** 18-34.

PEETERS, P. J., AERSSENS, J., DE HOOGT, R., STANISZ, A., GÖHLMANN, H. W., HILLSLEY, K., MEULEMANS, A., GRUNDY, D., STEAD, R. H. & COULIE, B. 2006. Molecular profiling of murine sensory neurons in the nodose and dorsal root ganglia labeled from the peritoneal cavity. *Physiol Genomics,* 24**,** 252-63.

RONG, W., HILLSLEY, K., DAVIS, J. B., HICKS, G., WINCHESTER, W. J. & GRUNDY, D. 2004. Jejunal afferent nerve sensitivity in wild-type and TRPV1 knockout mice. *The Journal of physiology,* 560**,** 867-881.

TORRES, J. L., PALOMINO, J., MORENO, R. D. & DE LOS REYES, M. 2017. Pannexin channels increase propidium iodide permeability in frozen-thawed dog spermatozoa. *Reprod Fertil Dev,* 29**,** 2269-2276.

WANG, R., BRAUGHTON, K. R., KRETSCHMER, D., BACH, T. H., QUECK, S. Y., LI, M., KENNEDY, A. D., DORWARD, D. W., KLEBANOFF, S. J., PESCHEL, A., DELEO, F. R. & OTTO, M. 2007. Identification of novel cytolytic peptides as key virulence determinants for community-associated MRSA. *Nat Med,* 13**,** 1510-4.

WHALEN, M. J., DALKARA, T., YOU, Z., QIU, J., BERMPOHL, D., MEHTA, N., SUTER, B., BHIDE, P. G., LO, E. H., ERICSSON, M. & MOSKOWITZ, M. A. 2008. Acute plasmalemma permeability and protracted clearance of injured cells after controlled cortical impact in mice. *Journal of cerebral blood flow and metabolism : official journal of the International Society of Cerebral Blood Flow and Metabolism,* 28**,** 490-505.